NUWC-NPT Technical Report 10,798
25 July 1997

Approximations to Directivity for Linear, Planar, and Volumetric Apertures and Arrays

Albert H. Nuttall
Surface Undersea Warfare Directorate

Benjamin A. Cray
Submarine Sonar Department

Naval Undersea Warfare Center Division
Newport, Rhode Island

PREFACE

This technical report was prepared by Benjamin A. Cray (Code 2133) and Albert H. Nuttall (Code 311) of the Naval Undersea Warfare Center (NUWC) for the Naval Sea Systems Command, Program Executive Office for Undersea Warfare (PEO-USW), Advanced Science and Technology Office (ASTO).

The work was sponsored by Michael Traweek (PEO-USW, ASTO). The NUWC assignment number was SS0124, with NUWC project number A198107. Some of the work described in this report was sponsored by the Independent Research (IR) Program of NUWC Division Newport under project number B100077, "Near-Optimum Detection of Random Signals with Unknown Locations, Structure, Extent, and Strengths," principal investigator Albert H. Nuttall. The IR program is funded by the Office of Naval Research.

The technical reviewer for this report was Sung H. Ko (Code 2133).

Reviewed and Approved: 25 July 1997

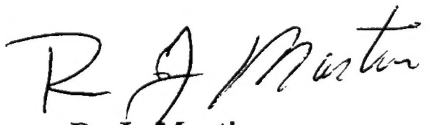

R. J. Martin
Head, Submarine Sonar Department

REPORT DOCUMENTATION PAGE

Form Approved
OMB No. 0704-0188

1. AGENCY USE ONLY *(Leave blank)*	2. REPORT DATE	3. REPORT TYPE AND DATES COVERED
	25 July 1997	FINAL

4. TITLE AND SUBTITLE

Approximations to Directivity for Linear, Planar, and Volumetric Apertures and Arrays

5. FUNDING NUMBERS

PE 0603013N
PE 0601152N

6. AUTHOR(S)

Albert H. Nuttall
Benjamin A. Cray

7. PERFORMING ORGANIZATION NAME(S) AND ADDRESS(ES)

Naval Undersea Warfare Center Division
1176 Howell Street
Newport, RI 02841-1708

8. PERFORMING ORGANIZATION REPORT NUMBER

TR 10,798

9. SPONSORING/MONITORING AGENCY NAME(S) AND ADDRESS(ES)

Naval Sea Systems Command
PEO-USW (ASTO)
2531 Jefferson Davis Highway
Arlington, VA 22242

Office of Naval Research
800 North Quincy St.
Arlington, VA 22217-5000

10. SPONSORING/MONITORING AGENCY REPORT NUMBER

11. SUPPLEMENTARY NOTES

12a. DISTRIBUTION/AVAILABILITY STATEMENT

Approved for public release; distribution is unlimited.

12b. DISTRIBUTION CODE

13. ABSTRACT *(Maximum 200 words)*

Even after decades of sonar design, approximations to the directivity factor or index of an array are often used inappropriately. Many of the approximations commonly used provide accurate directivity approximations for only the simplest of array geometries. As the array's size, shape, weighting, and complexity increase, there is a renewed need for better directivity approximations.

Directivity is defined as the ratio of the output signal-to-noise ratio (SNR) of an array to the input SNR at an omnidirectional element in a spherically isotropic noise field. Calculation of directivity is obtained by integrating the magnitude-squared response of the array over all angles of incidence. In spherical coordinates, these arrival angles are denoted by an azimuthal angle θ and a polar angle ϕ. Hence, calculation of the directivity requires a two-fold integration over the angular space defined by the azimuthal and polar angles. For complex, large-aperture arrays consisting of thousands of array elements, directivity calculations using numerical integration procedures can be time consuming, even on state-of-the-art computing systems. This report provides a number of accurate formulas for estimating the directivity of linear, planar, and volumetric apertures and arrays, which are allowed to have arbitrary amplitude shading coefficients, steering angles, and directional array element responses.

14. SUBJECT TERMS			15. NUMBER OF PAGES
Sonar Systems	Sonar Arrays	Conformal Arrays	65
Array Gain	Directivity	Directivity Index	16. PRICE CODE

17. SECURITY CLASSIFICATION OF REPORT	18. SECURITY CLASSIFICATION OF THIS PAGE	19. SECURITY CLASSIFICATION OF ABSTRACT	20. LIMITATION OF ABSTRACT
Unclassified	Unclassified	Unclassified	SAR

TABLE OF CONTENTS

LIST OF ILLUSTRATIONS

APPROXIMATIONS TO DIRECTIVITY FOR LINEAR, PLANAR, AND VOLUMETRIC APERTURES AND ARRAYS

1. INTRODUCTION

BACKGROUND

Even after decades of sonar design, approximations to the directivity factor or index of an array are sometimes used inappropriately. Many of the approximations commonly used provide accurate directivity approximations only for the simplest of array geometries. As the array's size, shape, weighting, and complexity increases, there is a renewed need for better directivity approximations.

Directivity is defined as the ratio of the output signal-to-noise power ratio (SNR) of an array to the input SNR at an omnidirectional element in a spherically isotropic noise field. Calculation of directivity requires integrating the magnitude-squared response of the array over all angles of incidence. In spherical coordinates, these arrival angles are denoted by an azimuthal angle θ and a polar angle ϕ. Hence, calculation of the directivity requires a two-fold integration over the angular space defined by the azimuthal and polar angles. For complex large-size arrays consisting of thousands of elements, directivity calculations using numerical integration procedures can be time consuming, even on state-of-the-art computing systems. This report provides a number of approximations for estimating the directivity of linear, planar, and volumetric arrays, which are allowed to have arbitrary real amplitude shading coefficients and element locations. The linear and planar arrays are allowed to have directional element responses as well.

A practical discussion of some of the well-known formulas for approximating directivity is given by Bobber[1], where the directivity factors (DFs) of three standard transducers are measured and compared to five theoretical methods used to calculate directivity. Two of the methods are based on approximations by Molloy[2], which use the simple formulas of $DF = 2L_e/\lambda$ for a line array with an effective aperture length of L_e, and $DF = 4\pi A_e/\lambda^2$ for a baffled planar array with an effective acoustic aperture area of A_e. For both cases, the effective aperture includes the physical array size plus half the array's interelement spacing at each end. In the free field, the planar array's directivity factor would be reduced by one-half.

These earlier approximations assumed an ideal model for the array response, where the mainlobe was relatively narrow (the length of the aperture exceeding several wavelengths) and the

peak sidelobe levels were much less than the mainlobe level. Furthermore, it was assumed that flat amplitude shading weights were applied to the individual array elements. Bobber does provide a short discussion on shading-weight correction factors that can be used, in some cases, to adjust the directivity factors. However, with current array configurations and signal processing, these earlier approximations are, in general, too limited.

GENERAL MODEL FOR ARRAY RESPONSE

For an array with arbitrary geometry and element locations, the beamformed array single-frequency amplitude response may be written as

$$A(\theta,\phi) = \sum_{n=1}^{N} w_n g_n(\theta,\phi) \exp(i(\vec{k} - \vec{k}_s) \cdot \vec{r}_n), \tag{1}$$

where $A(\theta,\phi)$ is the array's angular response to an arrival from azimuthal angle θ and polar angle ϕ; N is the total number of array elements; w_n and $g_n(\theta,\phi)$ are, respectively, the amplitude shading and element amplitude angular sensitivity of the n-th array element; $\vec{k}$ is the wavevector corresponding to an arriving acoustic planewave from (θ,ϕ); and $\vec{k}_s$ is the wavevector to which the array is steered. The corresponding steering angles are θ_s, ϕ_s. The n-th array element position is defined by the coordinate vector $\vec{r}_n = (x_n, y_n, z_n)$.

The linear, planar, and volumetric array coordinates are given in figure 1, along with the definition of spherical angles θ, ϕ.

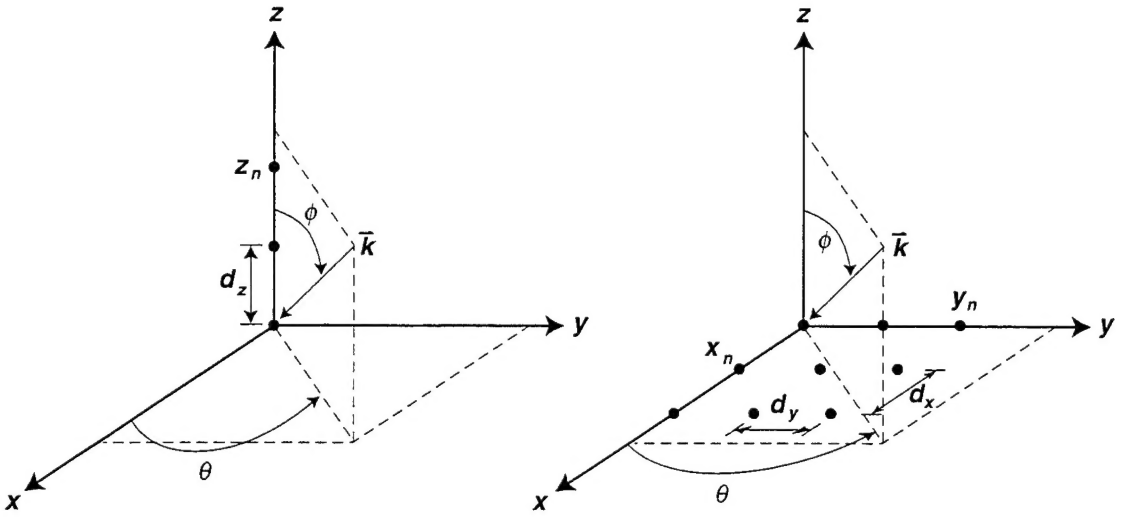

(a) Linear

(b) Planar

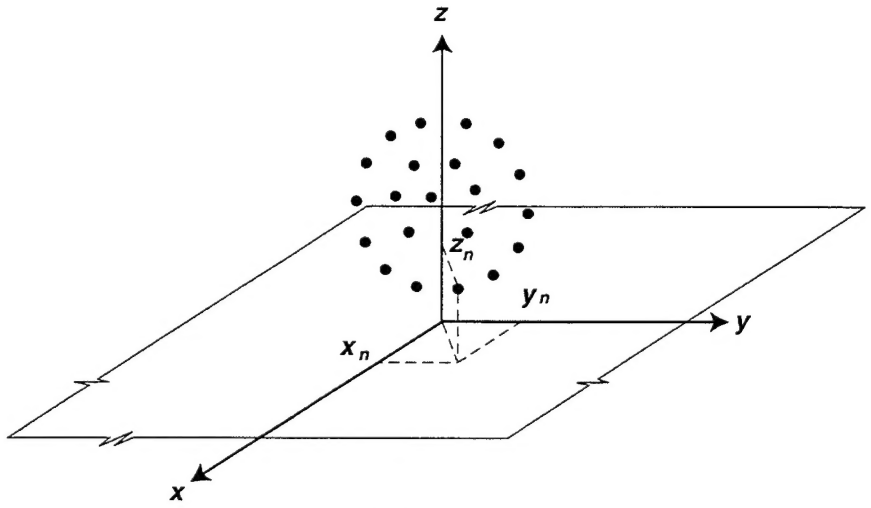

(c) Volumetric

Figure 1. Coordinate Systems for the Linear, Planar, and Volumetric Arrays

2. APPROXIMATIONS TO DIRECTIVITY

The directivity index (DI) is defined as a decibel measure of the improvement in the SNR that a beamformed array provides in an *ideal isotropic noise field* with a perfectly correlated signal, relative to an omnidirectional array element in the free field, i.e.,

$$DI = 10 \log DF = 10 \, Log \, \frac{(SNR)_{array\ output}}{(SNR)_{ff\ omni-element}}, \tag{2}$$

where DF is the directivity factor.

With the aid of equations (1) and (2), the components that comprise the calculation of the directivity index can be written as

$$S_{ff-omni} = S, \tag{3}$$

$$S_{array} = S\left|A(\theta_s, \phi_s)\right|^2, \tag{4}$$

$$N_{ff-omni} = \int_0^{2\pi} \int_0^{\pi} N_i \sin(\phi) d\phi \, d\theta, \tag{5}$$

and

$$N_{array} = \int_0^{2\pi} \int_0^{\pi} N_i \left|A(\theta, \phi)\right|^2 \sin(\phi) \, d\phi d\theta, \tag{6}$$

where S is defined as the received signal power level and N_i is defined as the isotropic noise power level.

Noting that equation (5) is simply $4\pi N_i$ and canceling the signal and isotropic noise power levels, the DF in equation (2) becomes

$$DF = \frac{4\pi \left|A(\theta_s, \phi_s)\right|^2}{\int_0^{2\pi} \int_0^{\pi} \left|A(\theta, \phi)\right|^2 \sin(\phi) d\phi d\theta}, \tag{7}$$

where $|A(\theta_s,\phi_s)|^2$ is the array power response at steering angle θ_s,ϕ_s.

Equations (6) and (7) indicate an integral with limits that account for all acoustic arrival angles. Hence, the directivity expression (equation (7)) assumes an unbaffled, or free-field, array configuration. In a baffled configuration, N_{array} would be reduced, resulting in an increased directivity.

The array amplitude response $A(\theta,\phi)$, given by equation (1), is for the most general three-dimensional array with arbitrary element locations, weights, and element responses. For this most general case, the sum of N terms can be evaluated only by calculating every individual complex term and summing up those N quantities. This is a particularly time-consuming task, especially when the number of elements N is large. When coupled with the fact that the DF requires computation of a double integral, namely equation (7), which must be repeated for each different frequency and/or steering angle, the computational burden often becomes excessive. Furthermore, as the number N of elements increases, the array power response $|A(\theta,\phi)|^2$ becomes even sharper in angles θ,ϕ, thereby requiring still finer evaluation of the integrand in equation (7) in order to retain accuracy in the final DF calculation. Hence, the need for accurate directivity approximations is obvious.

For the most general array configurations and processing, accurate directivity predictions can only be obtained by numerically integrating[3] the double integral given in equation (7). Also, for certain arrays, the maximum array power response $|A(\theta_m,\phi_m)|^2$ must be calculated and cannot be estimated. The maximum array response may not occur precisely at the steering angle (θ_s, ϕ_s) because of array curvature, unequal array element spacing, variable element sensitivities, and shading weights. This report, however, considers a broad set of array geometries and configurations which *may* be approximated, thereby avoiding the need for numerical integration.

DIRECTIVITY FACTORS FOR UNIFORM LINEAR ARRAYS

Approximating directivity plainly requires approximating the double integral in equation (7); the numerator typically can be determined directly from equation (1). In fact, for a line array with constant interelement spacing, the double integral in equation (7) may be evaluated exactly at the frequency for which spacing $d_z = \lambda/2$, regardless of the steering direction. This leads to

$$DI = 10\log\left\{\left(\sum_{n=1}^{N} w_n\right)^2 \Big/ \sum_{n=1}^{N} w_n^2\right\} \text{ independent of } \theta_s, \phi_s,$$

and for the special case of flat weighting, to the result

$$DI = 10\log\{N\} = 10\log\{2L_e/\lambda\}$$

for $d_z = \lambda/2$, as mentioned in section 1. Although this is an exact result for the uniform linear array, it is limited. For example, figure 2 illustrates the exact DF, obtained by numerical integration and normalized by the number of array elements, for an equispaced uniformly-weighted line array with nondirectional elements (uniform). For the frequency at which $f = f_o$, where $f_o(= c/2d_z)$ is the design frequency, the DF is independent of array steering and equals N. This is valid only at the design frequency f_o; as the line array's operating frequency changes, the DF becomes a function of frequency and steering angle. When $f < f_o$, a flare in the DF occurs near endfire, $\cos(\phi_s) \rightarrow \pm 1$, and results in a doubling of the DF precisely at endfire steering. This doubling results from the elimination of all grating lobes within the array response region. Equivalently, at these frequencies, the array response may be considered oversampled or overpopulated, $d_z/\lambda < 1/2$. Conversely, a droop in the DF occurs near endfire steering when $f > f_o$ because of the presence of grating lobes within the array response region. As the operating frequency increases above the design frequency, the droop occurs further from endfire; in fact, the breakpoint is approximately where $\left|\cos(\phi_s)\right| = 2f_o/f - 1 - 1/N$.

Derivations for the DF of more general linear arrays are presented in detail in the following pages. Subsequent approximations (for planar and volumetric arrays) follow the methodology outlined here and are less elaborate in their presentations.

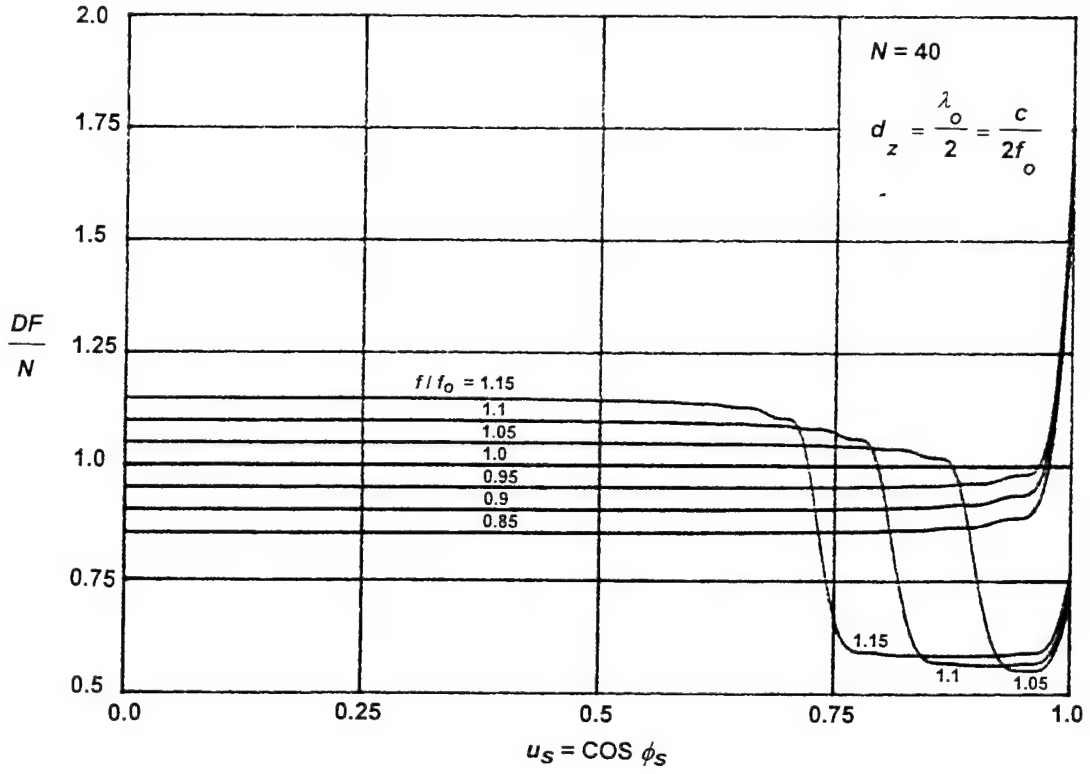

Figure 2. Normalized Directivity Factors for a Uniformly Weighted Equispaced Line Array

DISCRETE LINEAR ARRAYS

The line array is oriented along the z-axis, as shown in figure 1, and each array element is allowed to be directional. For example, the elements can have a common cosine angular dependence. The maximum angular response, or boresight, of these elements is chosen to be collinear to the y-axis. Therefore, the amplitude angular sensitivity becomes $g_n(\theta,\phi) = \left|\cos(\Theta)\right|^{\nu} = \left|\sin(\theta)\sin(\phi)\right|^{\nu}$, where $\Theta = (\theta,\phi)$ is the conical angle between the element's boresight and the planewave arrival angle, and ν is an arbitrary power to which the cosine is raised. For omnidirectional elements, $\nu = 0$. Figure 3 illustrates some typical element directionality patterns.

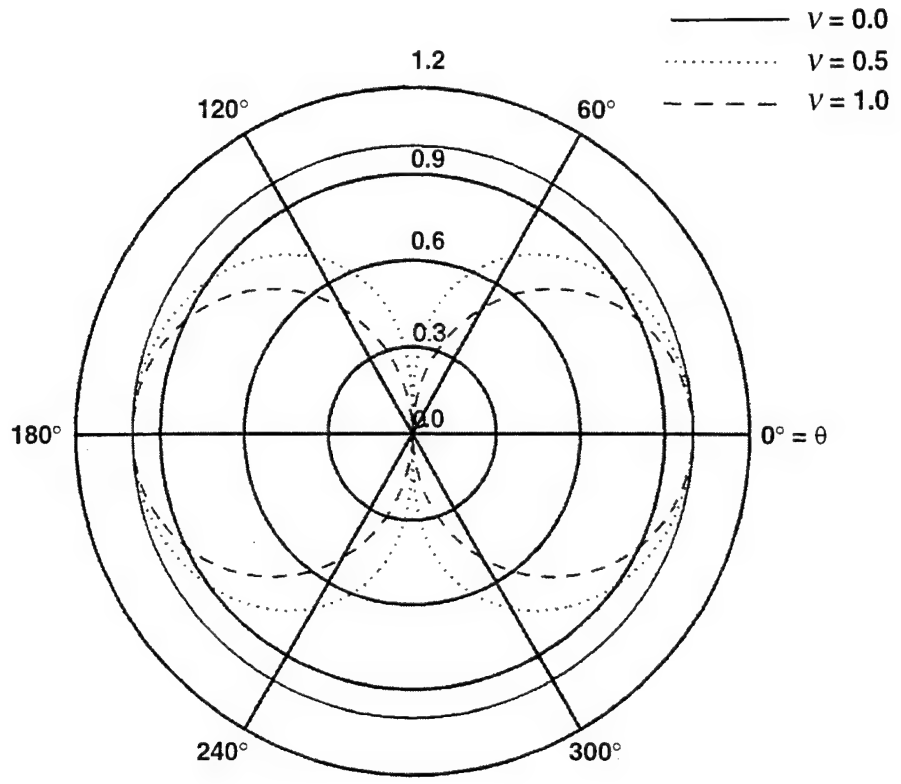

Figure 3. Element Angular Sensitivity $\left|\cos(\Theta)\right|^{\nu}$ ***for Powers*** ν ***= 0, 0.5, 1***

For the line array geometry, each element has the same angular dependence; that is, $g_n(\theta,\phi)$ is independent of n. Hence, from equation (1), the double integral in equation (7) becomes

$$I = \int_0^{2\pi}\int_0^{\pi}\left|\sum_{n=1}^{N} w_n\left|\sin(\theta)\sin(\phi)\right|^{\nu}\exp\left\{ikz_n(\cos(\phi)-\cos(\phi_s))\right\}\right|^2 \sin(\phi)\,d\phi\,d\theta. \tag{8}$$

Setting $u=\cos(\phi)$ and $u_s=\cos(\phi_s)$ yields

$$I = \int_0^{2\pi}\left\{\sin^2(\theta)\right\}^{\nu} d\theta \int_{-1}^{1}\left\{1-u^2\right\}^{\nu}\left|\sum_{n=1}^{N} w_n\exp\left\{ikz_n(u-u_s)\right\}\right|^2 du. \tag{9}$$

For integer ν, the integral over θ is straightforward; in fact, noninteger ν can be evaluated using gamma functions.[4] Thus, there follows

$$I = h(v)\int_{-1}^{1}(1-u^2)^v\left|\sum_{n=1}^{N} w_n \exp\{ikz_n(u-u_s)\}\right|^2 du, \tag{10}$$

where

$$h(v) = \frac{2^{(2v+1)}\Gamma^2(v+1/2)}{\Gamma(2v+1)} = 2\sqrt{\pi}\,\frac{\Gamma(v+1/2)}{\Gamma(v+1)}. \tag{11}$$

The simplification is obtained by the use of the duplication formula[5] for gamma functions. If it is assumed that the elements have a cosine angular dependence, then $v = 1$ and $h(1) = \pi$, whereas for omnidirectional elements, $v = 0$ and $h(0) = 2\pi$.

The focus here is on the behavior of the sum in equation (10) for large N. Using Lagrange's trigonometric identity, it is easily shown that for uniform weighting and equidistant element spacing d_z, the absolute value of the series sums to

$$\left|\sum_{n=1}^{N} \exp\{iknd_z(u-u_s)\}\right| = \left|\sin(Nkd_z(u-u_s)/2)/\sin(kd_z(u-u_s)/2)\right|. \tag{12}$$

The square of this sum, normalized by its maximum value N, is plotted in figure 4 along with the slowly varying u-function $1-u^2$ over the integration limits given in equation (10), for the case where $d_z = \lambda/2$ and $u_s = 0$.

It is apparent that the major contribution to the integral (10) occurs at $u = u_s$ and, provided that $u_s = \cos(\phi_s)$ is not close to ± 1 and that $d_z \le \lambda/2$, the contribution of the integrand function $1-u^2$ may be approximated at $u = u_s$. The integration in equation (10) then simplifies (for real weights) to

$$I \cong h(v)(1-u_s{}^2)^v \int_{-1}^{1} \sum_{n=1}^{N}\sum_{m=1}^{M} w_n w_m \exp\{i\alpha\pi(n-m)(u-u_s)\}du, \tag{13}$$

where α is a number proportional to half-wavelength spacing, i.e., $d_z = \alpha\lambda/2$. By interchanging the order of the u-integration with the summations, the integral can be evaluated exactly as

$$I \cong 2h(v)(\sin(\phi_s))^{2v} \times \left\{ \sum_{n=1}^{N} \sum_{m=1}^{M} w_n w_m \left\{ \delta_{nm} + (1-\delta_{nm}) \cos\left(\alpha\pi(n-m)\cos(\phi_s)\right) \frac{\sin\left(\alpha\pi(n-m)\right)}{\alpha\pi(n-m)} \right\} \right\}. \quad (14)$$

The Kronecker delta is denoted δ_{nm}. For half-wavelength element spacing, $\alpha = 1$ and equation (14) simplifies to

$$I \cong 2h(v)(\sin(\phi_s))^{2v} \sum_{n=1}^{N} w_n^2. \quad (15)$$

The maximum array response, in the direction the line array is steered, can be evaluated directly from equation (1) as

$$\left|A(\theta_s, \phi_s)\right|^2 = \sin^{2v}(\theta_s) \sin^{2v}(\phi_s) \left| \sum_{n=1}^{N} w_n \right|^2. \quad (16)$$

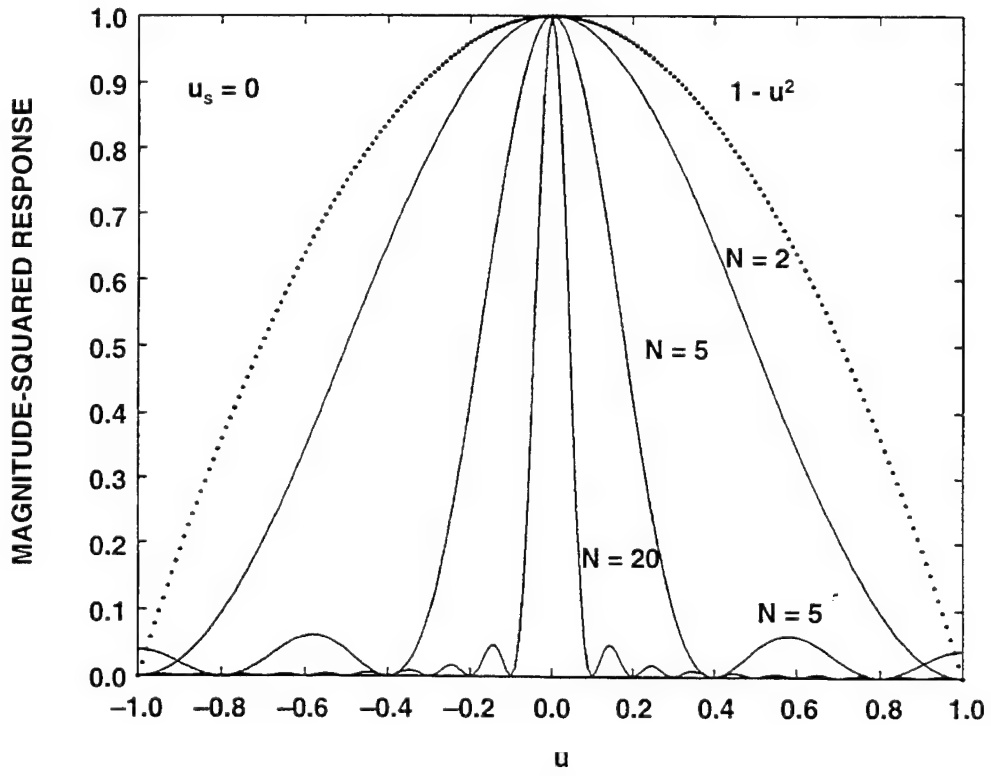

Figure 4. Comparison of the Slowly Varying Function 1- u^2 to the Function $\left| \sin(\frac{\pi}{2} Nu) \Big/ \left(N \sin(\frac{\pi}{2} u) \right) \right|^2$ **for** $N = 2, 5, 20$

Therefore, substitution of equations (14) and (16) into equation (7) yields the approximation for the DF of a linear array of equispaced *directional* elements having real, but arbitrary, shading weights, namely,

$$DF \cong \frac{2\pi \sin^{2\nu}(\theta_s)}{h(\nu)} \times \frac{\left|\sum_{n=1}^{N} w_n\right|^2}{\sum_{n=1}^{N}\sum_{m=1}^{M} w_n w_m \left\{\delta_{nm} + (1-\delta_{nm})\cos\left(\alpha\pi(n-m)\cos(\phi_s)\right)\frac{\sin\left(\alpha\pi(n-m)\right)}{\alpha\pi(n-m)}\right\}}. \tag{17}$$

The above expression could be written in terms of frequency using the substitution $\alpha = 2d_z f/c$, with f the operating frequency in Hertz and c the sound speed, provided that $f \le c/(2d_z) = f_o$.

For cosine element sensitivity $(\nu = 1)$ and half-wavelength element spacing, the DF in equation (17) simplifies to

$$DF \cong \frac{2\sin^2(\theta_s)\left|\sum_{n=1}^{N} w_n\right|^2}{\sum_{n=1}^{N} w_n^2} \equiv 2\sin^2\left(\theta_s\right)N_e, \tag{18}$$

where N_e is the effective number of weights. For the array element's maximum response, at $\theta_s = \pm\pi/2$ (in the y-axis direction), the cosine element sensitivity provides a doubling of the DF compared to that of an omnidirectional element. Thus, cosine element directivity can provide, at broadside, a 3-dB increase in the line array's DI.

Approximations for discrete linear arrays with nonperiodic element spacing (provided no interstitial array spacing is greater than half an acoustic wavelength) are derived in the following section as a special case of a weighted continuous linear aperture.

CONTINUOUS LINEAR APERTURES

For a continuously weighted linear aperture, the amplitude response for steering angle ϕ_s can be written as

$$A(\theta,\phi) = \int_{-\infty}^{\infty} w(z)g(z,\theta,\phi)\exp\{ikz(\cos(\phi)-\cos(\phi_s))\}dz, \tag{19}$$

where the real weighting $w(z)$ automatically terminates the integral at finite limits. This expression corresponds to the discrete array response shown in a general form by equation (1). Assuming, as in the discrete case, that this aperture has an amplitude angular sensitivity $g(\theta,\phi)$ (independent of z), which is proportional to a power of the cosine of the angle between the aperture's maximum response axis and the planewave arrival angle, then

$$A(\theta,\phi) = \left|\sin(\theta)\sin(\phi)\right|^{v} \int_{-\infty}^{\infty} w(z)\exp\{ikz(\cos(\phi)-\cos(\phi_s))\}dz. \tag{20}$$

For uniform angular response, the power is set to zero, $v = 0$.

Substituting equation (20) into the double integral in equation (7) and letting $u = \cos(\phi)$ as before, yields, after some simplification,

$$I = h(v)\int_{-1}^{1}(1-u^2)^{v}\left|\int_{-\infty}^{\infty} w(z)\exp\{ikz(u-u_s)\}dz\right|^2 du\,, \tag{21}$$

where $h(v)$ is defined by equation (11). Three steps are necessary to approximate this integral. First, as done in the discrete linear case, it is argued that $(1-u^2)^{v}$ varies slowly with u and that its contribution is well approximated by its value at $u = u_s$. Thus, for $|u_s| = |\cos(\phi_s)| < 1$,

$$I \cong h(v)(1-u_s^2)^{v}\int_{-1}^{1}\left|\int_{-\infty}^{\infty} w(z)e^{i\tau z}dz\right|^2 du, \tag{22}$$

where $\tau = k(u-u_s)$. The second step for the integral approximation considers the Fourier transform of the weighting function $w(z)$, which, by definition, is

$$W(\tau) = \int_{-\infty}^{\infty} w(z) e^{i\tau z} dz. \tag{23}$$

If it is presumed that the weighting $w(z)$ is even in z, then a Gaussian approximation for $W(\tau)$, which can be applied for *all* τ, is*

$$W(\tau) \cong W(0) \exp\left(-\frac{\tau^2}{2} m^2 \right), \tag{24}$$

where the mean-square length of weighting $w(z)$ is defined as

$$m^2 = \frac{\int_{-\infty}^{\infty} z^2 w(z) dz}{\int_{-\infty}^{\infty} w(z) dz}. \tag{24a}$$

This choice matches the moments of $w(z)$ through second order. Therefore, recognizing that the u-integration limits may now be extended to $\pm\infty$, equation (22) becomes

$$I \cong h(v) \left\{ \sin^2(\phi_s) \right\}^v W^2(0) \int_{-\infty}^{\infty} \exp\{-k^2 (u - u_s)^2 m^2\} du. \tag{25}$$

Finally, the integral in equation (25) may be evaluated exactly, yielding

$$I \cong h(v) \left\{ \sin^2(\phi_s) \right\}^v W^2(0) \frac{\sqrt{\pi}}{km}. \tag{26}$$

Thus, the approximation for the DF of a continuous line aperture, which is allowed to have nonuniform even weighting and a directional angular response, is

$$DF \cong \frac{8\pi^{3/2} \sin^{2v}(\theta_s)}{h(v)} \frac{m}{\lambda} = 4\sqrt{\pi} \frac{m}{\lambda} \left[\frac{\sqrt{\pi} \Gamma(v+1) \sin^{2v}(\theta_s)}{\Gamma(v+1/2)} \right]. \tag{27}$$

---

*An alternative approach for a linear aperture is given in appendix A.

The quantity $m = \left\{\int_{-\infty}^{\infty} z^2 w(z)dz\right\}^{1/2} \Big/ \left\{\int_{-\infty}^{\infty} w(z)dz\right\}^{1/2}$ in equation (27) may be interpreted as the root-mean-square (RMS) length of weighting $w(z)$.

For maximum directivity, the best value for steering angle θ_s is $\theta_s = \pm\pi/2$ (along the y-axis). It is illustrative to consider the v-dependence of the bracketed term (shading factor) in equation (27) on directivity. Recall that as v increases, the aperture's angular response becomes narrower. Figure 5 plots the bracketed term in equation (27) for various fixed values of steering angle θ_s. Notice that for the steering angle $\theta_s = \pi/2$, the function starts at unity for $v = 0$ and increases monotonically with v. Given this choice of steering angle, it is seen that the DF increases with element directivity. However, any other choice of steering angle leads to an eventual decay of the DF with v. This implies that in general, highly directional elements will result in a gain in directivity along the element's boresight, but with the cost of a significant decrease in directivity for other steering angles.

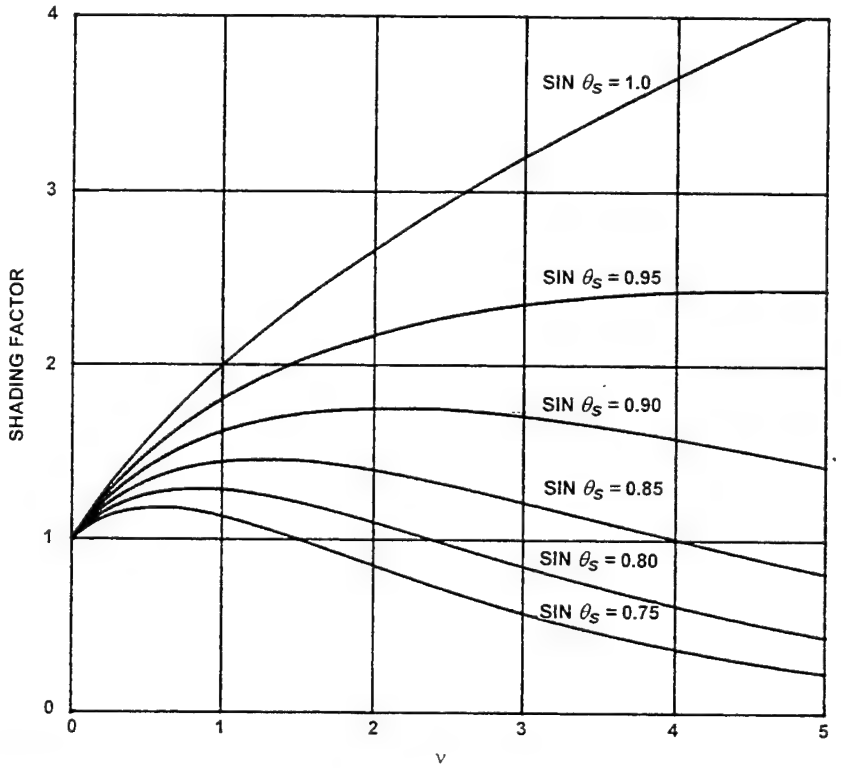

Figure 5. Shading Factor for Line Aperture with $|\cos(\Theta)|^v$ Element Directionality

It should be noted that the DF in equation (27) is independent of polar steering angle ϕ_s and, hence, of $\sin(\phi_s)$. More generally, it may be shown that if the element amplitude response

$g(z,\theta,\phi)$ in equation (19) varies slowly with angle and is independent of position z, then equation (27) is replaced by

$$DF \cong 4\sqrt{\pi}\frac{m}{\lambda}\frac{2\pi g^2(\theta_s,\phi_s)}{\int_0^{2\pi} g^2(\theta,\phi_s)d\theta}. \tag{27a}$$

The latter factor is obviously unity for a flat angular response $g(\theta,\phi)$. If the angular response is separable, that is, $g(\theta,\phi)=g_1(\theta)g_2(\phi)$, the approximate DF simplifies to

$$DF \cong 4\sqrt{\pi}\frac{m}{\lambda}\frac{2\pi g_1^2(\theta_s)}{\int_0^{2\pi} g_1^2(\theta)d\theta}, \tag{27b}$$

which is independent of the polar angular dependence $g_2(\phi)$. This independence of the DF on the element directivity will also appear in the derivations for the planar and volumetric apertures. The special result in equation (27) corresponds to $g_1(\theta)=|\sin(\theta)|^{\nu}$ and any slowly varying $g_2(\phi)$. For a uniform angular aperture response, $\nu=0$, equation (27) simplifies to

$$DF \cong 4\sqrt{\pi}\frac{m}{\lambda}. \tag{28}$$

From equation (27) or equation (28), it is straightforward to obtain an approximation for the directivity of a *discrete* line array having arbitrary element locations $\{z_n\}$, provided that no interstitial element spacing is greater than a half-wavelength and the origin of coordinates is located so that $\sum_{n=1}^{N} w_n z_n = 0$. For example, a discrete line array of N elements has an impulsive weighting function

$$w(z)=\sum_{n=1}^{N} w_n \delta(z-z_n). \tag{29}$$

Substituting this weighting function into equations (24a) and (28) gives

$$DF \cong \frac{4\sqrt{\pi}}{\lambda}\frac{\left\{\sum_{n=1}^{N} w_n z_n^2\right\}^{1/2}}{\left\{\sum_{n=1}^{N} w_n\right\}^{1/2}}. \tag{30}$$

DIRECTIVITY FACTORS FOR PLANAR APERTURES

The approximation $4\pi A_e/\lambda^2$ for the DF of an equispaced baffled planar array, where A_e is the effective array area, is only applicable for an array having ideal half-omnidirectional elements, flat weighting, and broadside steering. These restrictions can be eliminated by using the Gaussian approximation technique described above for the continuous linear aperture.

The amplitude response for a continuous planar aperture with arbitrary real weighting (which need not be separable) and lying in the xy-plane is

$$A(\theta,\phi) = \left|\cos(\phi)\right|^{v} \int_{-\infty}^{\infty}\int_{-\infty}^{\infty} w(x,y)\exp\{ik\sin(\phi)[x\cos(\theta)+y\sin(\theta)] - ik\sin(\phi_s)[x\cos(\theta_s)+y\sin(\theta_s)]\}dxdy, \tag{31}$$

where it is presumed that the aperture's amplitude directionality is proportional to a cosine to a power, with the maximum response or boresight aligned along the z-axis, $\phi = 0$, namely, broadside to the aperture. The geometry is illustrated in figure 1b. A uniform or omnidirectional aperture angular response corresponds to $v = 0$. Again, the weighting function $w(x,y)$ terminates the integral and defines an effective finite aperture. Equation (31) may be written more compactly by introducing the multidimensional Fourier transform

$$W(u,v) = \int_{-\infty}^{\infty}\int_{-\infty}^{\infty} w(x,y)\exp\{iux+ivy\}dxdy. \tag{32}$$

Now let $u = \sin(\phi)\cos(\theta)$ and $v = \sin(\phi)\sin(\theta)$. Then, the planar aperture amplitude response becomes

$$A(\theta,\phi) = \left|\cos(\phi)\right|^{v} W(ku-ku_s, kv-kv_s).$$

Evaluation of the double integral in equation (7) requires a one-to-one mapping of the $\theta\phi$-plane into the uv-plane. The Jacobian of the transformation is

$$\frac{\partial(u,v)}{\partial(\theta,\phi)} = \cos(\phi)\sin(\phi). \tag{33}$$

To prevent a two-to-one mapping, the upper limit on the ϕ-integral in equation (7) must be decreased to $\phi_2 = \pi/2$. This change in the limit is possible because the planar aperture response is symmetric about the *xy*-plane (see equation (31)). This observation allows for the change in the upper limit, and the ϕ-integral is simply doubled; if the integral over $(0,\pi/2)$ is not multiplied by two, the resultant DF will be for an ideally baffled planar array. With this change, the integration region in the $\theta\phi$-plane maps to the interior of a unit circle C_1 in the *uv*-plane. Thus, from equations (31) to (33), the denominator of equation (7) becomes

$$I = 2\iint_{C_1} (1-u^2-v^2)^{\nu-1/2} \left|W(ku-ku_s, kv-kv_s)\right|^2 dudv. \tag{34}$$

The peak of the integrand in the *uv*-plane occurs at (u_s, v_s), namely at radius $\sqrt{u_s^2+v_s^2} = \sin(\phi_s)$. If $\sin(\phi_s) < 1$, that is, $\phi_s < \pi/2$ or steered to the upper hemisphere, then $\cos(\phi_s) > 0$ and the integral may be approximated in the manner described earlier, namely,

$$I \cong \frac{2(\cos^2(\phi_s))^{\nu-1/2}}{k^2} \int_{-\infty}^{\infty}\int_{-\infty}^{\infty} \left|W(u,v)\right|^2 dudv. \tag{35}$$

The Gaussian approximation for the double Fourier transform of the (even) weighting function $w(x,y)$ (as in equation (24) for the continuous line aperture) is*

$$W(u,v) \cong W(0,0)\exp\left(-\frac{u^2}{2}m_x^2 - \frac{v^2}{2}m_y^2\right), \tag{36}$$

where mean square lengths

$$m_x^2 = \frac{\int_{-\infty}^{\infty}\int_{-\infty}^{\infty} x^2 w(x,y)dxdy}{\int_{-\infty}^{\infty}\int_{-\infty}^{\infty} w(x,y)dxdy}, \quad m_y^2 = \frac{\int_{-\infty}^{\infty}\int_{-\infty}^{\infty} y^2 w(x,y)dxdy}{\int_{-\infty}^{\infty}\int_{-\infty}^{\infty} w(x,y)dxdy}. \tag{36a}$$

Substituting the Gaussian approximation into equation (35) and performing the *uv*-integration yields

*An alternative approach for a planar aperture is given in appendix A.

$$I \cong \frac{(\cos^2(\phi_s))^{\nu-1/2} W^2(0,0)\lambda^2}{2\pi m_x m_y} \tag{37}$$

for the denominator of equation (7), where it has been assumed that $m_x >> \lambda$ and $m_y >> \lambda$. Hence, the DF for an unbaffled planar aperture is

$$DF \cong 8\pi^2 \cos(\phi_s)\frac{m_x m_y}{\lambda^2} \tag{38}$$

for $\phi_s < \pi/2$, which is independent of power ν. The quantity $m_x m_y$ may be interpreted as the RMS aperture area in the *xy*-plane.

More generally, if the factor $|\cos(\phi)|^\nu$ in equation (31) is replaced with a slow angular dependence $g(\theta,\phi)$, as in equation (19), it may be shown that *exactly* the same result for the DF (equation (38)) is obtained. The approximate planar DF is independent of a general slowly varying angular response $g(\theta,\phi)$. The $\cos(\phi_s)$ dependency in equation (38) results from the foreshortening of the planar aperture in the *xy*-plane when seen from the polar angle ϕ_s; it has nothing to do with the aperture's angular sensitivity. The reason for the independence on angular sensitivity, $g(\theta,\phi)$, or on parameter ν, for a planar aperture is due to its ability to resolve in *both* θ and ϕ. The narrow resolution of the planar aperture response $A(\theta,\phi)$ quickly overcomes that of the relatively broad and slowly varying angular response $g(\theta,\phi)$; this assumes, of course, that ν is of moderate order for dependency $\left|\cos(\Theta)\right|^\nu$.

As an example of approximating the directivity, consider the simple case of a nondirectional, uniformly weighted rectangular aperture steered to broadside ($\phi_s = 0$). Letting L_x and L_y be the physical lengths of the aperture in the *x*- and *y*-directions, respectively, then $m_x = L_x/(2\sqrt{3})$ and $m_y = L_y/(2\sqrt{3})$. Thus, the DF becomes

$$DF \cong 2\pi^2 \frac{L_x L_y}{3\lambda^2} = \frac{\pi}{3} 2\pi \frac{L_x L_y}{\lambda^2}. \tag{39}$$

The well-known approximation for an unbaffled planar array steered to broadside and having uniform weights is $DF \cong 2\pi A_e/\lambda^2$, where $A_e = L_x L_y$ (see appendix A). Therefore, the above Gaussian approximation is 5 percent larger, giving roughly 0.2-dB greater DI.

Extending the Gaussian approximation for directivity (equation (38)), to *discrete* equispaced planar arrays presents no complications, provided that the array spacings are not greater than half an acoustic wavelength $(d_x, d_y) \le \lambda/2$. For instance, the weighting function for an equispaced rectangular planar array may be expressed as

$$w(x,y) = \sum_{n=1}^{N}\sum_{m=1}^{M} w_{nm}\,\delta\!\left(x - d_x\left[n - \frac{N+1}{2}\right]\right)\delta\!\left(y - d_y\left[m - \frac{M+1}{2}\right]\right), \tag{40}$$

where w_{nm} need not be separable in n and m. From equations (36a) and (38), the directivity factor for the discrete equispaced unbaffled planar array follows immediately as

$$DF \cong \frac{8\pi^2 d_x d_y \cos(\phi_s)}{\lambda^2} \frac{\left\{\sum_{n=1}^{N}\sum_{m=1}^{M} w_{nm}\left[n - \frac{N+1}{2}\right]^2\right\}^{1/2}\left\{\sum_{n=1}^{N}\sum_{m=1}^{M} w_{nm}\left[m - \frac{M+1}{2}\right]^2\right\}^{1/2}}{\sum_{n=1}^{N}\sum_{m=1}^{M} w_{nm}} \tag{41}$$

for $\phi_s < \pi/2$.

For flat weights, expression (41) simplifies to the compact form

$$DF = \frac{\pi}{3} 2\pi\cos(\phi_s)\frac{d_x d_y}{\lambda^2}\left(N^2-1\right)^{1/2}\left(M^2-1\right)^{1/2}.$$

If $d_x\left(N^2-1\right)^{1/2}/12^{1/2}$ is interpreted as the RMS length m_x of the array in the x direction (with a similar interpretation in the y direction), this expression for DF simplifies to $8\pi^2\cos(\phi_s)m_x m_y/\lambda^2$, which is identical to the DF given for the unbaffled planar aperture in equation (38). The quantity $\left(N^2-1\right)^{1/2}$ behaves as $N - 1/(2N)$ for large N, leading to $m_x \sim d_x N/12^{1/2}$.

More generally, for arbitrary element locations, the weighting function is given by $w(x,y) = \sum_{t=1}^{T} w_t\,\delta(x - x_t)\delta(y - y_t)$, where T is the total number of elements and locations $\{x_t, y_t\}$ are arbitrary, except that no interstitial array spacings can exceed a half-wavelength.

DIRECTIVITY FACTORS FOR VOLUMETRIC APERTURES

Exact expressions for the directivity of a solid spherical volumetric aperture and a spherical shell are given by Anderson.[6] For values of $D/\lambda >> 1$, where D is the diameter of the sphere, the expressions for the DFs yield the approximations

$$DF_{solid} \cong 8.7\left(\frac{D}{\lambda}\right)^2 \tag{42}$$

and

$$DF_{shell} \cong 12.6\left(\frac{D}{\lambda}\right)^{1.8}. \tag{43}$$

These expressions are for continuously distributed elements that are uniformly weighted and nondirectional. The exact DF for a thick shell of inner and outer radii of r_1 and r_2, respectively, follows readily from the procedure in reference (6), although not done there. Here, the authors' approximation procedure (to be derived) yields the form

$$DF \cong \frac{16\pi^2}{5\lambda^2}\frac{r_2^4 + r_2^3 r_1 + r_2^2 r_1^2 + r_2 r_1^3 + r_1^4}{r_2^2 + r_2 r_1 + r_1^2}. \tag{44}$$

For a solid spherical aperture, $r_1 = 0$, and for a shell, $r_1 = r_2$. Thus, the authors' Gaussian approximations are

$$DF_{solid} \cong \frac{4\pi^2}{5}\frac{D^2}{\lambda^2} \approx 7.9\frac{D^2}{\lambda^2} \tag{45}$$

and

$$DF_{shell} \cong \frac{4\pi^2}{3}\frac{D^2}{\lambda^2} \approx 13.16\frac{D^2}{\lambda^2}. \tag{46}$$

These approximations compare reasonably well with equations (42) and (43), respectively.

The approximate DF derived below allows for arbitrary volumetric shapes, element positions, and shading weights; however, the elements must remain nondirectional. For certain volumetric geometries, such as a cylinder or sphere, it may be possible to allow element

directionality, although the derivations are likely to be extremely difficult. Furthermore, a baffle may be introduced in the volumetric aperture so that steerings and planewave arrival directions are restricted to the upper hemisphere (see figure 1c); the volumetric aperture does not, in general, have a symmetric response about the *xy*-plane.

The derivation of the approximate DF here follows closely the Gaussian approximation for the continuous planar aperture. The amplitude response of a general continuous volumetric aperture is

$$A(\theta,\phi) = \int_{-\infty}^{\infty}\int_{-\infty}^{\infty}\int_{-\infty}^{\infty} \overline{w}(x,y,z)\exp\{ik[x\cos(\theta)\sin(\phi) + y\sin(\theta)\sin(\phi) + z\cos(\phi)] - ik[x\cos(\theta_s)\sin(\phi_s) + y\sin(\theta_s)\sin(\phi_s) + z\cos(\phi_s)]\}dxdydz, \tag{47}$$

where $\overline{w}(x,y,z)$ is a general three-dimensional continuous real weighting function. Notice that the angular response of the aperture itself is assumed omnidirectional. Defining the triple Fourier transform

$$\overline{W}(u,v,w) = \int_{-\infty}^{\infty}\int_{-\infty}^{\infty}\int_{-\infty}^{\infty} \overline{w}(x,y,z)\exp\{iux + ivy + iwz\}dxdydz \tag{48}$$

for all u,v, and w, allows the amplitude response to be recast in the form

$$A(\theta,\phi) = \overline{W}(k\sin(\phi)\cos(\theta) - ku_s, k\sin(\phi)\sin(\theta) - kv_s, k\cos(\phi) - kw_s) \tag{49}$$

for $0 \le \theta \le 2\pi$, $0 \le \phi \le \pi$, where $u_s = \sin(\phi_s)\cos(\theta_s)$, $v_s = \sin(\phi_s)\sin(\theta_s)$, and $w_s = \cos(\phi_s)$. Note that the amplitude response in the steered direction (θ_s, ϕ_s) is simply

$$A(\theta_s,\phi_s) = \overline{W}(0,0,0) = \int_{-\infty}^{\infty}\int_{-\infty}^{\infty}\int_{-\infty}^{\infty} \overline{w}(x,y,z)dxdydz. \tag{50}$$

Substituting equation (49) into the double integral in equation (7) and employing the same variable transform and arguments used to develop equations (32) to (34) gives, for the denominator of equation (7),

$$I = \iint_{C_1} \frac{dudv}{\sqrt{1-u^2-v^2}} \left| \overline{W}\left(ku - ku_s, kv - kv_s, k\sqrt{1-u^2-v^2} - k\sqrt{1-u_s^2-v_s^2}\right) \right|^2 . \tag{51}$$

Note that equation (51), unlike equation (34), is not multiplied by 2 and thus corresponds to a *baffled* volumetric aperture, which responds only in the upper hemisphere, $\phi < \pi/2$.

A new obstacle for the volumetric aperture is the quantity $\sqrt{1-u^2-v^2}$, which appears in $\overline{W}$. This quantity would become imaginary for $u^2+v^2>1$; hence, a small-order expansion about u_s and v_s is introduced. That is, let $u = u_s + \varepsilon$ and $v = v_s + \delta$. Equation (51) then becomes

$$I = \iint_{C_s} \frac{d\varepsilon d\delta}{\sqrt{1-(u_s+\varepsilon)^2-(v_s+\delta)^2}} \left| \overline{W}(k\varepsilon, k\delta, kQ(\varepsilon,\delta)) \right|^2 , \tag{52}$$

where $Q(\varepsilon,\delta) = \sqrt{1-(u_s+\varepsilon)^2-(v_s+\delta)^2} - \sqrt{1-u_s^2-v_s^2}$ and C_s is a unit circle centered at $(\varepsilon,\delta) = (-u_s,-v_s)$. The term $Q(\varepsilon,\delta)$ can be linearly approximated by invoking a binomial expansion and neglecting terms of second order in ε and δ. Thus, $Q(\varepsilon,\delta) \cong -(u_s\varepsilon + v_s\delta)/w_s$ for small ε,δ.

For symmetric and real weighting function $\overline{w}(x,y,z)$, the Gaussian approximation of $\overline{W}(u,v,w)$ for all u, v, and w (as in equation (36) for a planar aperture) is written as

$$\overline{W}(u,v,w) \cong \overline{W}(0,0,0)\exp\left(-\frac{u^2}{2}m_x^2 - \frac{v^2}{2}m_y^2 - \frac{w^2}{2}m_z^2\right), \tag{53}$$

where

$$m_x^2 = \frac{\int_{-\infty}^{\infty}\int_{-\infty}^{\infty}\int_{-\infty}^{\infty} x^2\overline{w}(x,y,z)dxdydz}{\int_{-\infty}^{\infty}\int_{-\infty}^{\infty}\int_{-\infty}^{\infty} \overline{w}(x,y,z)dxdydz}, \quad m_y^2 = \frac{\int_{-\infty}^{\infty}\int_{-\infty}^{\infty}\int_{-\infty}^{\infty} y^2\overline{w}(x,y,z)dxdydz}{\int_{-\infty}^{\infty}\int_{-\infty}^{\infty}\int_{-\infty}^{\infty} \overline{w}(x,y,z)dxdydz},$$

and

$$m_z^2 = \frac{\int_{-\infty}^{\infty}\int_{-\infty}^{\infty}\int_{-\infty}^{\infty} z^2\overline{w}(x,y,z)dxdydz}{\int_{-\infty}^{\infty}\int_{-\infty}^{\infty}\int_{-\infty}^{\infty} \overline{w}(x,y,z)dxdydz}. \tag{53a}$$

Using this Gaussian approximation, it follows that

$$\left|\overline{W}(k\varepsilon,k\delta,k\underline{Q}(\varepsilon,\delta))\right|^2 \cong \overline{W}^2(0,0,0)\exp\left(-k^2\varepsilon^2 m_x^2 - k^2\delta^2 m_y^2 - k^2\frac{(\varepsilon u_s+\delta v_s)^2}{w_s^2}m_z^2\right) \tag{54}$$

for all ε,δ. Substituting equation (54) into equation (52), and recognizing that the limits of integration may now be extended to $\pm\infty$, yields

$$I \cong \frac{1}{w_s}\int_{-\infty}^{\infty}\int_{-\infty}^{\infty}\overline{W}^2(0,0,0)\exp\left[-\frac{\alpha}{2}\varepsilon^2 - \frac{\beta}{2}\delta^2 + \gamma\varepsilon\delta\right]d\varepsilon d\delta, \tag{55}$$

where $\alpha = 2k^2\left(m_x^2 + m_z^2u_s^2/w_s^2\right)$, $\beta = 2k^2\left(m_y^2 + m_z^2v_s^2/w_s^2\right)$, and $\gamma = -2k^2\left(m_z^2u_sv_s/w_s^2\right)$. The integrals in equation (55) may be evaluated exactly[4], provided that $\alpha>0$, $\beta>0$, and $\alpha\beta>\gamma^2$; thus, the denominator of equation (7) is

$$\begin{aligned} I &\cong \frac{\pi\overline{W}^2(0,0,0)}{k^2\sqrt{m_x^2m_y^2w_s^2 + m_x^2m_z^2v_s^2 + m_y^2m_z^2u_s^2}} \\ &= \frac{\overline{W}^2(0,0,0)}{4\pi}\frac{\lambda^2}{\sqrt{m_x^2m_y^2\cos^2(\phi_s) + m_x^2m_z^2\sin^2(\phi_s)\sin^2(\theta_s) + m_y^2m_z^2\sin^2(\phi_s)\cos^2(\theta_s)}}. \end{aligned} \tag{56}$$

Then, from equation (7), the DF for a baffled volumetric aperture is approximated as

$$DF \cong \frac{16\pi^2}{\lambda^2}\sqrt{m_x^2m_y^2\cos^2(\phi_s) + m_x^2m_z^2\sin^2(\phi_s)\sin^2(\theta_s) + m_y^2m_z^2\sin^2(\phi_s)\cos^2(\theta_s)}, \tag{57}$$

where it is assumed that m_x, m_y, and m_z are all significantly greater than a wavelength.

The product m_xm_y above may be considered the RMS effective area of the collapsed weighting in the *xy*-plane, that is,

$$m_xm_y = \left[\frac{\int_{-\infty}^{\infty}x^2\,\mathrm{w}_x(x)dx}{\int_{-\infty}^{\infty}\mathrm{w}_x(x)dx}\frac{\int_{-\infty}^{\infty}y^2\,\mathrm{w}_y(y)dy}{\int_{-\infty}^{\infty}\mathrm{w}_y(y)dy}\right]^{1/2}, \tag{58}$$

where $w_x(x) = \int_{-\infty}^{\infty} \int_{-\infty}^{\infty} \overline{w}(x,y,z)dydz$ and $w_y(y) = \int_{-\infty}^{\infty} \int_{-\infty}^{\infty} \overline{w}(x,y,z)dxdz$. Notice that the term $\cos(\phi_s)$, which is multiplied by the product $m_x m_y$ in equation (57), is the cosine of the angle between the steering direction and the normal to the *xy*-plane (consider a unit steering vector $\vec{e} = \vec{e}_x \cos(\theta_s)\sin(\phi_s) + \vec{e}_y \sin(\theta_s)\sin(\phi_s) + \vec{e}_z \cos(\phi_s)$; then $\vec{e} \cdot \vec{e}_z = \cos(\phi_s)$). Thus, the RMS area of the collapsed weighting in the *xy*-plane, *as seen from the steering direction*, is

$$A_{xy} = m_x m_y \left|\cos(\phi_s)\right|. \tag{59}$$

In a similar manner, the RMS areas of the collapsed weightings in the other planes are

$$A_{xz} = m_x m_z \left|\sin(\theta_s)\sin(\phi_s)\right|, \tag{60}$$

$$A_{yz} = m_y m_z \left|\cos(\theta_s)\sin(\phi_s)\right|. \tag{61}$$

Hence, the baffled volumetric directivity approximation, equation (57), returns to the familiar form

$$DF \cong \frac{16\pi^2 A_e}{\lambda^2} = \frac{16\pi^2}{\lambda^2}\left(A_{xy}^2 + A_{xz}^2 + A_{yz}^2\right)^{1/2}, \tag{62}$$

where A_e is the RMS effective aperture area for the given steering direction θ_s, ϕ_s.

As an example, consider a continuous flat weighting function, $\overline{w}(x, y, z) = \text{constant}$, for a cubic volumetric aperture $|x| < L_x/2$, $|y| < L_y/2$, and $|z| < L_z/2$. Then, from equation (53a),

$$m_x = \frac{L_x}{2\sqrt{3}}, \qquad m_y = \frac{L_y}{2\sqrt{3}}, \qquad m_z = \frac{L_z}{2\sqrt{3}}. \tag{63}$$

The effective RMS area is given as

$$A_e = \frac{1}{12}\left(L_x^2 L_y^2 \cos^2(\phi_s) + L_x^2 L_z^2 \sin^2(\theta_s)\sin^2(\phi_s) + L_y^2 L_z^2 \cos^2(\theta_s)\sin^2(\phi_s)\right)^{1/2}, \tag{64}$$

and the approximate directivity of the baffled cubic aperture with flat weighting becomes

$$DF \cong \frac{4\pi^2}{3\lambda^2}\left(L_x^2 L_y^2 \cos^2(\phi_s) + L_x^2 L_z^2 \sin^2(\theta_s)\sin^2(\phi_s) + L_y^2 L_z^2 \cos^2(\theta_s)\sin^2(\phi_s)\right)^{1/2}. \tag{65}$$

As expected, for $L_z = 0$ and $\phi_s = 0$, equation (65) reduces immediately to twice the value of equation (39), the approximate directivity of a uniformly weighted nondirectional planar aperture in the free field (not baffled).

Equation (57) can be extended to include discrete, rather than continuous, array elements using an impulsive weighting function; that is,

$$\overline{w}(x,y,z) = \sum_{t=1}^{T} \overline{w}_t\, \delta(x - x_t)\, \delta(y - y_t)\, \delta(z - z_t). \tag{66}$$

The general case is found directly by substituting equation (66) into the integrals in equation (53a) and evaluating the Gaussian approximation for the volumetric DF given by equation (57).

The approximation for the DF of a volumetric aperture was derived by using a Gaussian approximation for the magnitude-squared response. The result, equation (57), uses the RMS lengths of the collapsed weightings in the various dimensions. As shown in appendix A, alternative approaches for linear and planar apertures, which used the Parseval relation, yielded approximations to the DF that depended on *effective* lengths or areas, respectively, of the weightings. The analogous derivation for a volumetric aperture or array has not been discovered. Nevertheless, by extension, the following conjectured form for the directivity of a volumetric *array* with equal element spacing d in all three dimensions, based upon the earlier results for the linear and planar arrays, is offered (see appendix B).

If $\{w_{xyz}(n,m,k)\}$ are the three-dimensional weights applied to the equispaced volumetric array, the three collapsed (or projected) two-dimensional weight structures are defined as

$$w_{xy}(n,m) = \sum_k w_{xyz}(n,m,k), \quad w_{xz}(n,k) = \sum_m w_{xyz}(n,m,k), \quad w_{yz}(m,k) = \sum_n w_{xyz}(n,m,k). \tag{67}$$

The three *effective* numbers of weights are then defined according to

$$N_{xy} = \frac{\left[\sum_{nm} w_{xy}(n,m)\right]^2}{\sum_{nm} w_{xy}^2(n,m)}, \qquad N_{xz} = \frac{\left[\sum_{nk} w_{xz}(n,k)\right]^2}{\sum_{nk} w_{xz}^2(n,k)}, \qquad N_{yz} = \frac{\left[\sum_{mk} w_{yz}(m,k)\right]^2}{\sum_{mk} w_{yz}^2(m,k)}. \tag{68}$$

The *conjectured* directivity at operating frequency f for a volumetric array is then given by

$$DF = 4\pi \frac{d^2}{\lambda^2} N_e = \pi \frac{f^2}{f_o^2}\left[N_{xy}^2 w_s^2 + N_{xz}^2 v_s^2 + N_{yz}^2 u_s^2\right]^{1/2}. \tag{69}$$

Here, $f_o = c / (2d)$ is the design frequency, where the common element spacing d is a half-wavelength. The steering parameters are $u_s = \sin(\phi_s)\cos(\theta_s)$, $v_s = \sin(\phi_s)\sin(\theta_s)$, and $w_s = \cos(\phi_s)$.

3. COMPARISON WITH EXACT RESULTS

In this section, comparisons are made between the exact DF (computed by numerical integration) and an approximate DF, for a variety of weighted linear, planar, and volumetric arrays. In most cases, Hanning weighting is employed, and the array elements are nondirectional.

Section 2 gave Gaussian approximations for the DFs of various arrays. However, the Gaussian approach only matches the mainlobe region of the array power response and takes no account of the sidelobes, which may be very significant. An alternative approach, specifically for arrays, that *does* take into account both the mainlobe *and* the sidelobes is presented in appendix B. This latter approximate procedure has been found to be more accurate and is used for all the numerical examples in this section. As will be seen, the approximations are quite accurate, even for arrays with relatively few elements and steered near endfire. With increasing array size, the approximations become more accurate, which is just when approximations are most beneficial; that is, numerical integration can become time consuming and burdensome for large arrays.

LINEAR ARRAY

Figure 6 shows that for the equispaced line array with spacing d and steering parameter $u_s = \cos \phi_s = 0.2$, the approximation for the DF is valid beyond $f = f_o$; in fact, the fit is good up to $f = 1.6 f_o$. This result corresponds to element spacing $d = 1.6\ \lambda/2$, that is, greater then half-wavelength spacing. This behavior occurs because smaller values of $|u_s|$ keep the closest grating lobe of the array response at greater distances from the visible region, thereby allowing the approximation to have wider applicability. In fact, the approximation is valid for $d < \lambda/(1 + |u_s|)$, which corresponds to $f/f_o < 2/(1 + |u_s|)$. For $u_s = 0.2$, the latter bound is $f/f_o < 1.67$, which is in good agreement with figure 6. For the equispaced line array with $u_s = 0.8$, the bound is $f/f_o < 1.1$, which agrees well with figure 7, especially for the larger values of N.

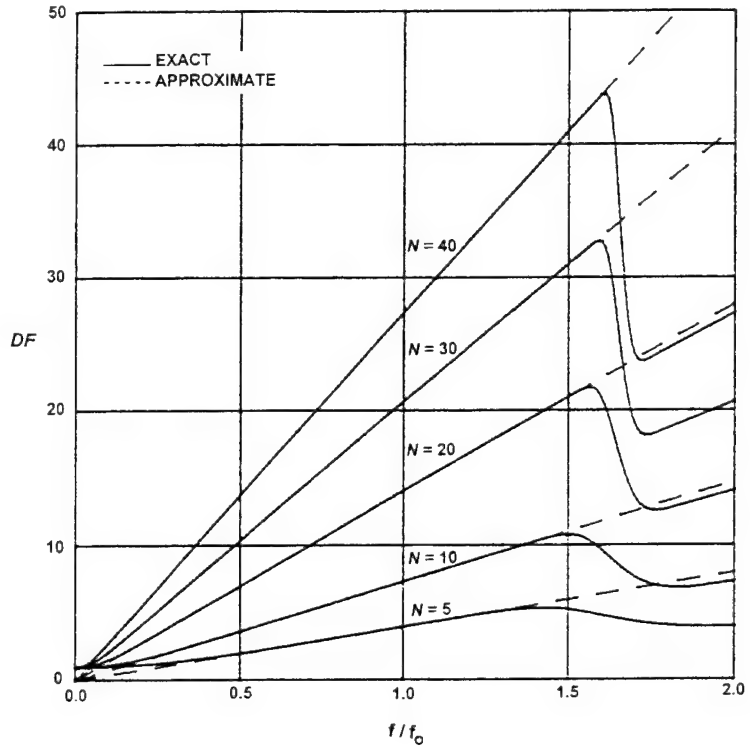

Figure 6. DF for an Equispaced Line Array with Hanning Weighting, $u_s = 0.2$

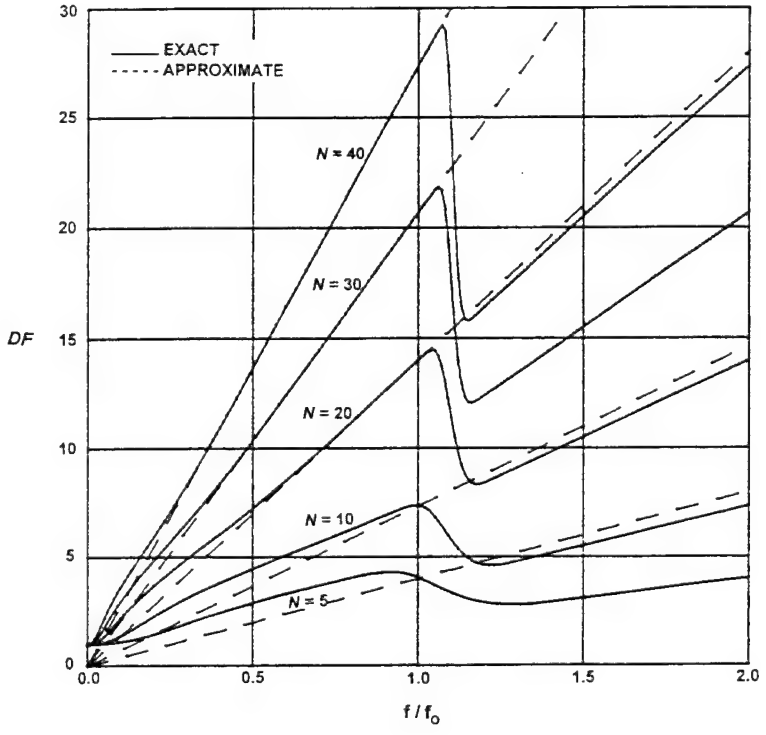

Figure 7. DF for an Equispaced Line Array with Hanning Weighting, $u_s = 0.8$

An example of a 40-element line array with directional amplitude response $|\sin(\theta)\sin(\phi)|$, that is, power $v = 1$, is given in figure 8. Because both the exact result and the approximation for the DF involve steering angle θ_s only through the multiplicative term $\sin^2(\theta_s)$, this common quantity is factored off; this leads to a plot of $\mathrm{DF}/\sin^2(\theta_s)$, which depends only on the remaining polar steering angle ϕ_s.

For polar steering angle ϕ_s near 0 or π (endfire steering), the parameter $u_s = \cos\phi_s$ is near ± 1. The approximate DF is not as accurate in this case for two reasons. The function $(1-u^2)^v$ varies fastest at the edges of the integration range (-1, 1) on u, thereby making its extraction from the integral as $(1-u_s^2)^v$ less accurate. Also, the sidelobes of $|W(ku-ku_s)|^2$ can extend significantly beyond $u = 1$ if u_s is near +1 (beyond $u = -1$ if u_s is near -1); these sidelobes would not be encountered in the exact integral for V over (-1, 1). However, the aproximating integral for V extends over all the sidelobes on both sides of the mainlobe, halfway up to the next grating lobe.

This lack of accuracy for ϕ_s near 0 and π is illustrated in figures 8 and 9, where the discrepancy of the exact DF from the approximate DF is significant even when $f/f_o < 1$, that is, $d < \lambda/2$. The errors are less for Hanning weighting than for flat weighting because Hanning sidelobes decay to low levels faster, tending to minimize the two effects discussed above. Of course, for both weightings, the approximate DF only applies for $f/f_o < 2/(1+|u_s|)$ or $d/\lambda < 1/(1+|u_s|) = 1/(1+|\cos(\phi_s)|)$, at which point grating lobes begin to manifest themselves.

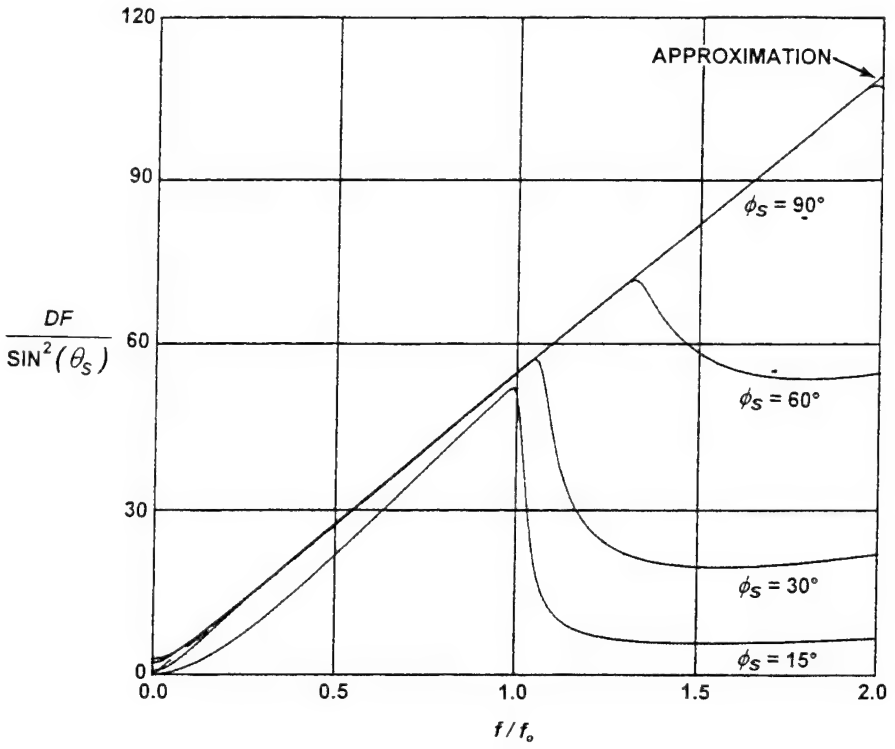

Figure 8. DF for an Equispaced Line Array with Hanning Weighting, $N = 40$, $\nu = 1$

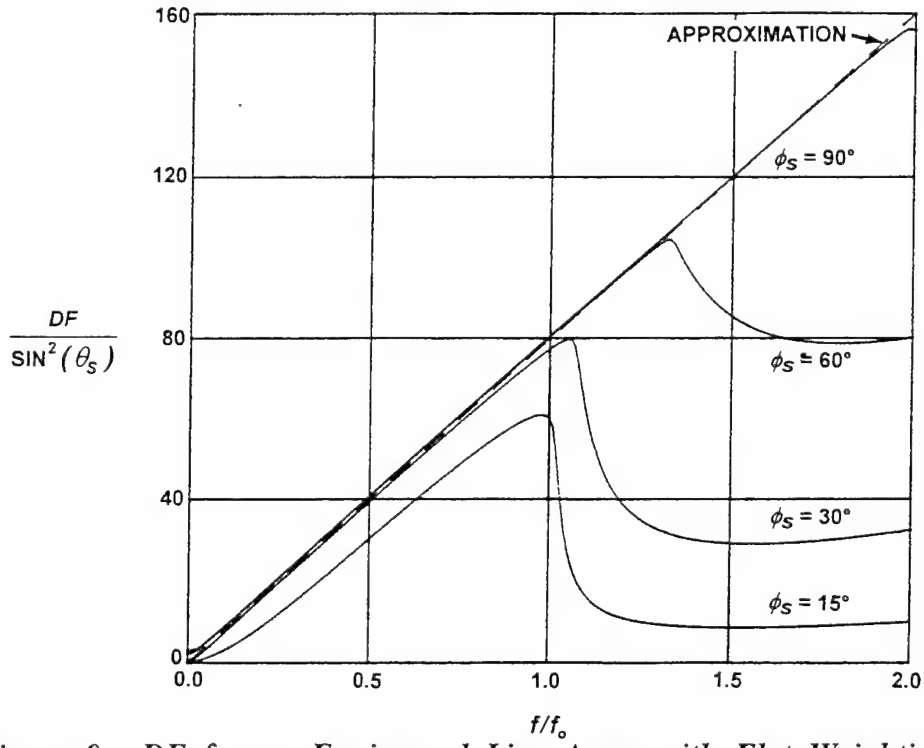

Figure 9. DF for an Equispaced Line Array with Flat Weighting, $N = 40$, $\nu = 1$

The next example consists of a curved line array, specifically an equispaced semicircular array centered at the origin in the *xy*-plane with its middle element located on the *x*-axis; that is, the angular locations of the N elements are

$$\theta_n = -\frac{\pi}{2} + \pi \frac{n-1}{N-1}$$

for $1 \le n \le N$. The elements are all located at radius r and employ flat weighting. Although this case might be considered a (sparse) planar array, its DF behaves like that of a line array, being linearly proportional to the effective curved line length, namely,

$$DF \equiv \frac{2}{\lambda} L_e \equiv \frac{2}{\lambda} \pi r \frac{N}{N-1} = 2\pi \frac{N}{N-1} \frac{r}{\lambda}.$$

(The factor $N/(N-1)$ represents the effective extension of the edge elements, when the weighting is flat.) The approximate DF is plotted as a dashed line in figure 10 and agrees very well with the exact results for several polar steering angles. The tic mark labeled "H" indicates where the distance between adjacent elements is a half-wavelength; the approximate DF is excellent for smaller spacings, despite the fact that the sidelobes of this particular unweighted array are rather poor (~ -8 dB). The breakpoint between the approximation and exact results is located approximately where the spacing/wavelength ratio is $2/(1+|u_s|) = 2/(1+\sin\phi_s)$ for this example where azimuth steering angle $\theta_s = 0$.

The only difference in figure 11 is that azimuthal steering angle θ_s is changed to $\pi/2$, that is, along the *y*-axis. Again, the approximate DF above is excellent when the spacing/wavelength ratio is less than $2/\left(1+\max\{|u_s|,|v_s|\}\right) = 2/\left(1+\sin\phi_s\right)$ for $\theta_s = \pi/2$.

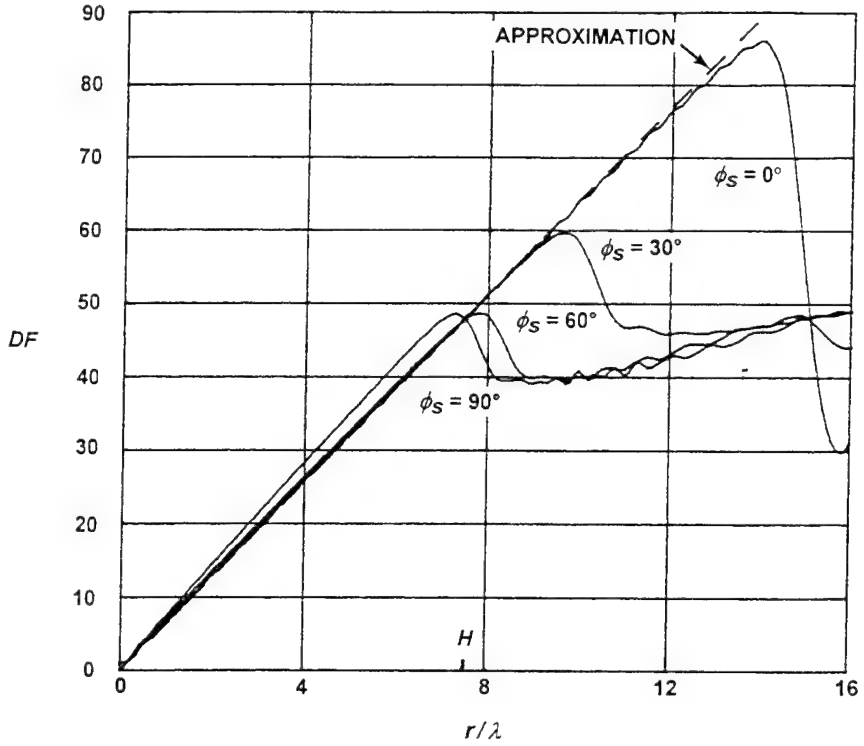

Figure 10. DF for an Equispaced Semicircle Array with Flat Weighting, $N = 48$, $\theta_s = 0$

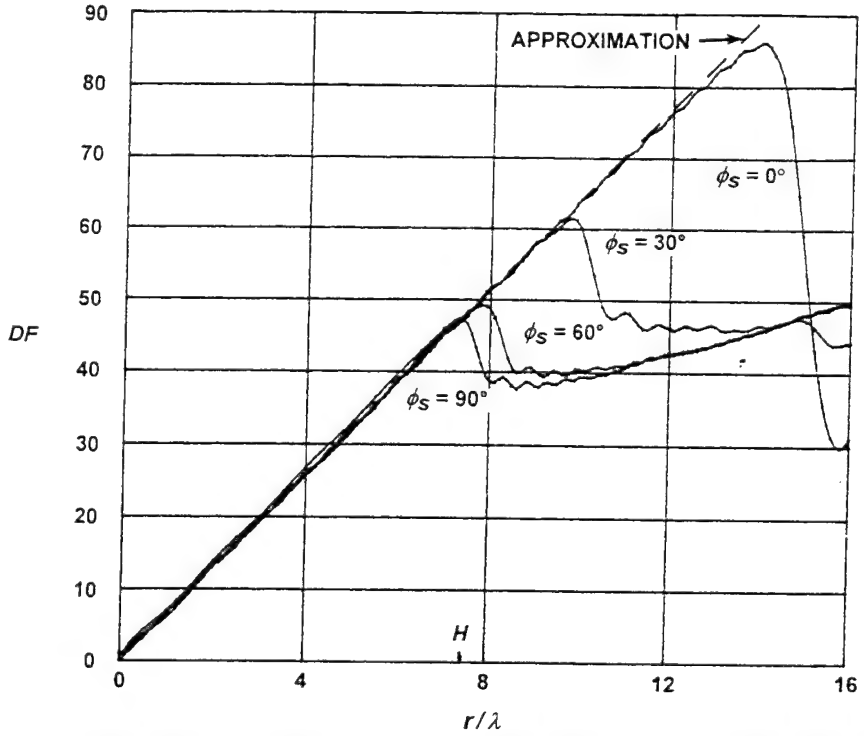

Figure 11. DF for an Equispaced Semicircle Array with Flat Weighting, $N = 48$, $\theta_s = \pi / 2$

PLANAR ARRAY

For a *baffled* planar array with elements spaced at distance d in *both* the x and y dimensions, the upper bound on operating frequency f, for which the DF approximation is valid, is

$$\frac{f}{f_0} < \frac{2}{\left(1-a^2\right)^{1/2} + b},$$

where $a = \min(|u_s|, |v_s|)$, $b = \max(|u_s|, |v_s|)$. This result agrees well with the baffled planar array results in figures 12 and 13. A more accurate bound is given in appendix B.

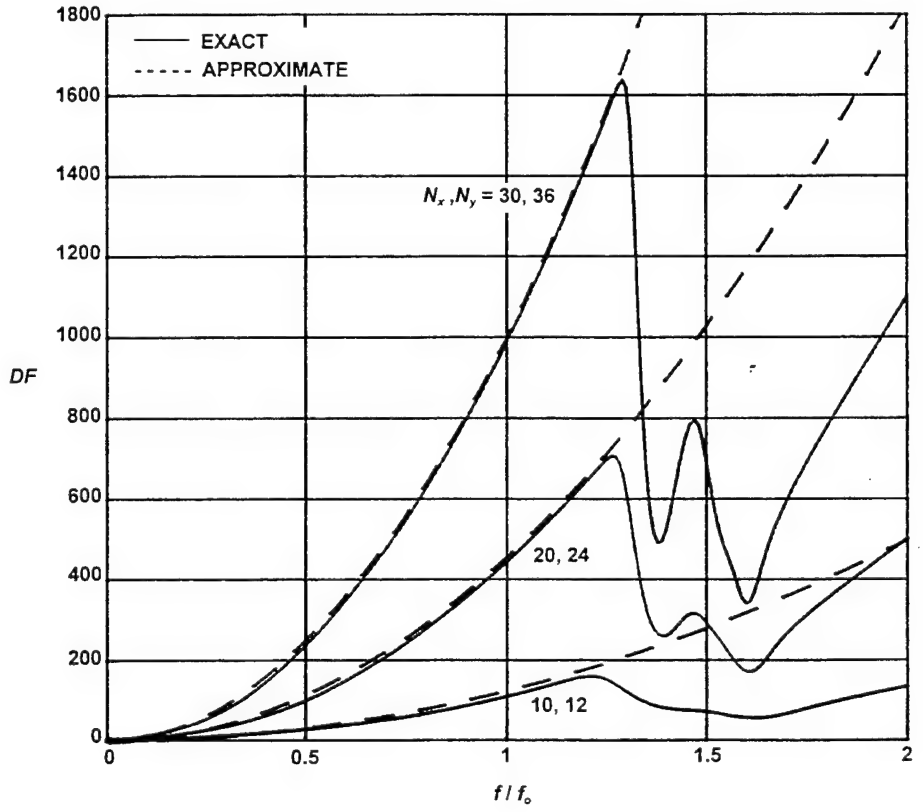

Figure 12. DF for an Equispaced Baffled Planar Array with Multiplicative Hanning Weighting, $d_x = d_y$, $u_s = 0.5$, $v_s = 0.6$

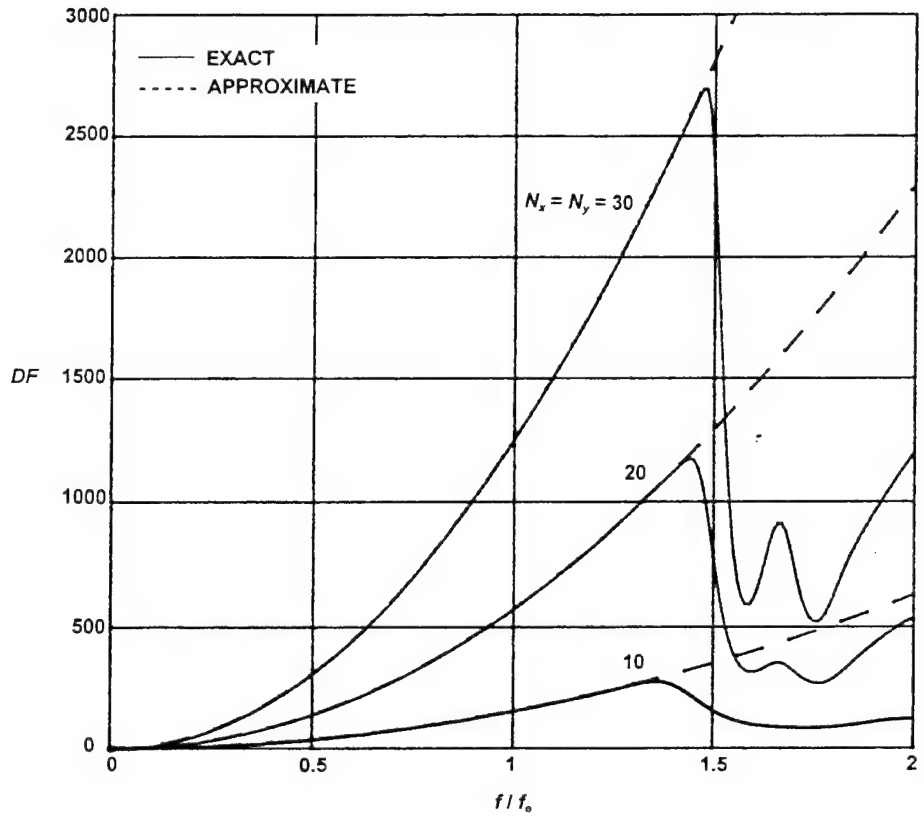

Figure 13. DF for an Equispaced Baffled Planar Array with Multiplicative Hanning Weighting, $d_x = d_y$, $u_s = 0.2$, $v_s = 0.3$

VOLUMETRIC ARRAY

An example of the application of the DF approximation (equation (69)) is given in figure 14 for an equispaced volumetric array with multiplicative Hanning weighting w_{xyz} in the three dimensions. The numbers of elements are $N_x = 10$, $N_y = 12$, $N_z = 15$, and the steering direction is $u_s = 0$, $v_s = 0$, $w_s = 1$; that is, toward the North Pole.

Results for an unbaffled, as well as a baffled, volumetric array are presented in figure 14 (solid curves), along with the directivity approximation (dashed curve). The agreement between the exact baffled DF and the conjectured DF is excellent up to approximately $f/f_o = 1.8$, whereas the exact unbaffled DF differs significantly in the neighborhood of $f/f_o = 1$ and for $f/f_o > 1.7$.

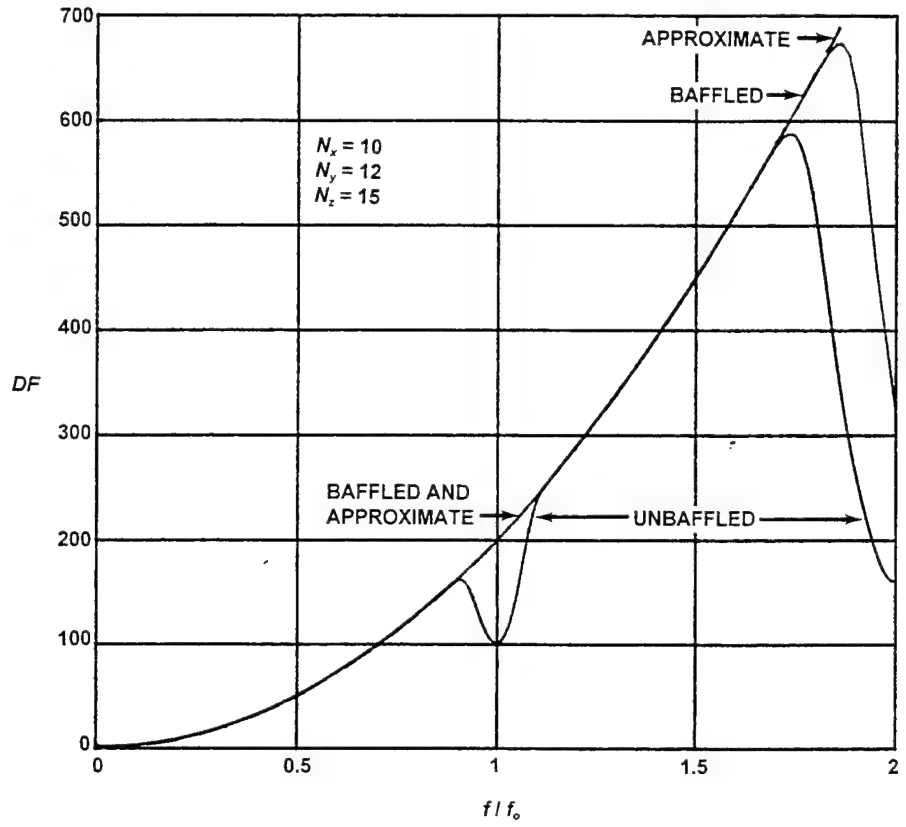

Figure 14. DF for an Equispaced Volumetric Array with Multiplicative Hanning Weighting, $u_s = 0$, $v_s = 0$, $w_s = 1$

These differences occur because of the locations of the aliasing lobes of the unbaffled volumetric array. For the present equispaced array with common separation distance d in three dimensions and *separable* weighting, the array function is given by the product of three functions of the form

$$\sum_{n=1}^{N_x} w_{xn} \exp\left[inkd\left(u - u_s\right)\right], \qquad kd = \pi \frac{f}{f_o}. \tag{70}$$

The y and z functions are similar, with replacements v - v_s and w - w_s, respectively, inside the exponential. This function of u has period $2\pi / (kd) = 2f_o / f$, with the desired mainlobe at $u = u_s$. The remaining aliasing lobes at $u = u_s \pm m2f_o / f$ can become major grating lobe contributors under conditions to be developed below.

If the double integral on θ, ϕ in equation (7) is interpreted as a triple integral in u, v, w space, the integration takes place only *on the unit sphere*. Therefore, significant contributions to

he integral can take place only when the three array functions have combinations of mainlobes and at least one aliasing lobe that intersect *on the sphere*. For example, one such case is

$$u_s^2 + v_s^2 + \left[w_s - 2\frac{f_o}{f} \right]^2 = 1; \quad \text{that is,} \quad \frac{f}{f_o} = \frac{1}{|w_s|}. \tag{71}$$

More generally, the frequencies at which a significant contribution occurs to the double integral in equation (7), and only *one* aliasing lobe is involved, are

$$\frac{f}{f_o} = \frac{1}{|u_s|} \quad \text{or} \quad \frac{1}{|v_s|} \quad \text{or} \quad \frac{1}{|w_s|}. \tag{72}$$

When two aliasing lobes are involved, the interfering frequencies are

$$\frac{f}{f_o} = \frac{2}{|u_s| + |v_s|} \quad \text{or} \quad \frac{2}{|u_s| + |w_s|} \quad \text{or} \quad \frac{2}{|v_s| + |w_s|}. \tag{73}$$

Finally, when three aliasing lobes are involved (no mainlobes), the interfering frequencies are

$$\frac{f}{f_o} = \frac{3}{|u_s| + |v_s| + |w_s|}. \tag{74}$$

In general, the lowest frequency at which grating lobes contribute, for an unbaffled equispaced volumetric array, is

$$\frac{f_{\min}}{f_o} = \frac{1}{\max\{|u_s|, |v_s|, |w_s|\}}. \tag{75}$$

For example, in figure 14, with u_s, v_s, w_s = 0, 0, 1, the problematical frequencies for an unbaffled array are $f/f_o = 1 / w_s = 1$ and $2 / (u_s+w_s) = 2$, at least for $0 \le f/f_o \le 2$. The lower frequency corresponds to a lower-hemisphere response at $w = w_s - 2f_o/f = 1-2 = -1$. Because the baffled array cannot respond in the lower hemisphere, it has no major response at $f/f_o = 1$, thereby maintaining the larger value of directivity, in agreement with the approximate DF (which ignores grating lobes).

The width of the discrepancy between exact and approximate DFs is related to the beamwidth of the array in the angular dimensions. Larger numbers of elements will lead to narrower beamwidths and therefore, narrower regions of discrepancy between the unbaffled array DF and the approximate DF.

The top example in figure 15 uses an unbaffled volumetric array with N_x, N_y, N_z = 20, 24, 30 elements, respectively, and steering direction u_s, v_s, w_s = 0.6, 0.4, 0.693. The lowest interfering frequency occurs at $f/f_o = 1 / w_s = 1.44$, due to the aliasing lobe at $w = w_s - 2f_o/f =$ -0.693. This is a lower-hemisphere response.

The next lowest frequency is $f/f_o = 2/(u_s + w_s) = 1.55$. The contributing lobes are at $u = u_s - 2f_o/f = -0.693$, $v = v_s = 0.4$, and $w = w_s - 2f_o/f = -0.6$. Notice that the sum of squares of these three locations is 1, meaning on the unit sphere. This is also a lower-hemisphere response.

The next frequency is $f/f_o = 1/u_s = 1.67$. The contributing lobes are at $u = u_s - 2f_o/f = -0.6$, $v = v_s = 0.4$, and $w = w_s = 0.693$. This is an upper-hemisphere response. (For a baffled array, this would be the lowest frequency leading to an aliased response.)

Finally, there are two other responses that blend together, namely $f/f_o = 3 / (u_s + v_s + w_s)$ = 1.77 and $2 / (v_s + w_s) = 1.83$. The aliasing lobe locations are at $u = u_s - 2f_o/f =$ -0.53, $v = v_s - 2f_o/f =$ -0.73, $w = w_s - 2f_o/f =$ -0.437 for the first case, and at $u = u_s = 0.6$, $v = v_s - 2f_o/f$ = -0.693, $w = w_s - 2f_o/f =$ -0.4 for the second case. Both of these cases are lower-hemisphere responses.

The bottom unbaffled example in figure 15 uses eight times fewer elements, namely 1800 elements instead of 14,400. The decreased resolution capability causes several of the aliased responses to overlap, making it impossible to identify individual aliased contributions.

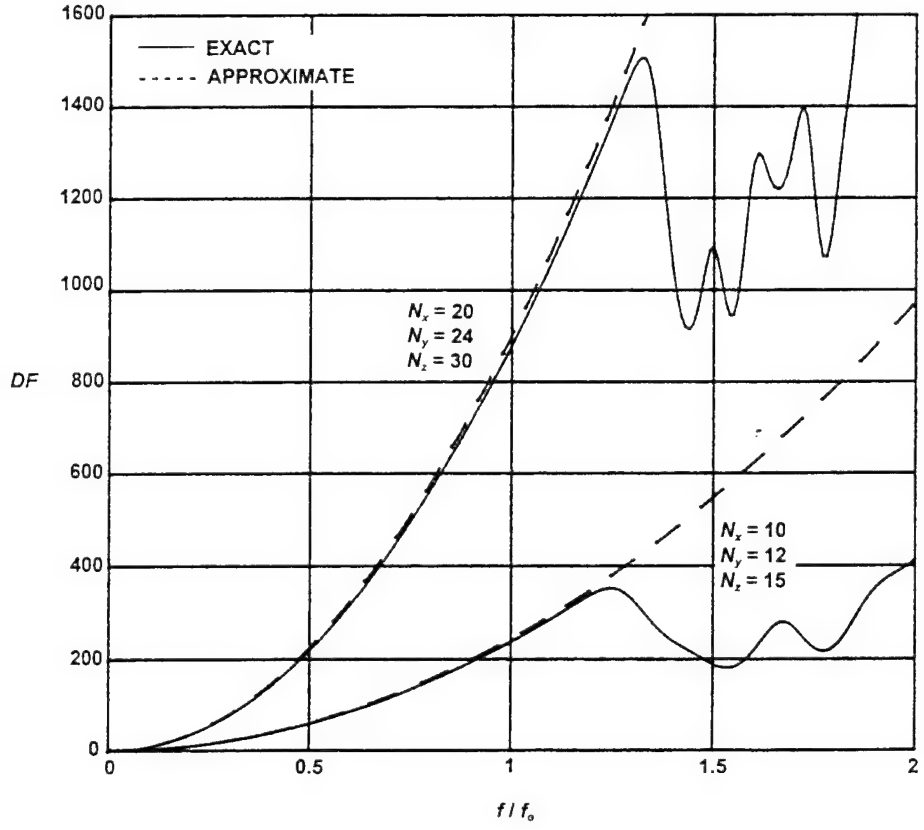

Figure 15. DF for an Equispaced Unbaffled Volumetric Array with Multiplicative Hanning Weighting, u_s = 0.6, v_s = 0.4, w_s = 0.693

APPLICABILITY TO VOLUMETRIC ARRAYS, BAFFLED AND UNBAFFLED

Although there is only one form for the approximate DF of a volumetric array, this form has different ranges of applicability, depending on whether baffling is used. The approximate DF takes no account of grating lobes, whereas actual arrays are always subject to the effects of grating lobes. This is evident in figure 14, where the agreement of the approximate DF with the exact baffled DF is excellent up to $f/f_o = 1.8$, whereas the agreement with the exact unbaffled DF holds only up to $f/f_o = 0.9$. Baffling suppresses all the lower-hemisphere grating lobes; the dip in the unbaffled DF near $f/f_o = 1$ is due to a lower-hemisphere grating lobe which is responding to undesired noise arrivals. However, it should be noted that for frequencies $1.1 < f/f_o < 1.7$, the approximate DF again agrees with the exact unbaffled DF; this occurs because the particular grating lobe in figure 14 only contributes in the neighborhood of $f/f_o = 1$.

The general frequencies at which an equispaced unbaffled volumetric array is subject to a grating lobe are

$$\frac{f}{f_o} = \frac{I^2 + J^2 + K^2}{|u_s I + v_s J + w_s K|}, \tag{76}$$

where I, J, and K are positive and negative integers, not all equal to zero. The lowest frequency was given earlier in equation (75).

For an equispaced *baffled* volumetric array, not all the frequencies in equation (76) lead to grating lobes. To determine which frequencies are relevant, a search over all the small integer values for I, J, and K, such as 0, ±1, ±2, must first be conducted. Then, those cases corresponding to negative values of $w_s + K 2 f_o / f$ must be discarded, because they correspond to lower-hemisphere grating lobes, which will not be active in a baffled application. The remaining cases constitute valid grating lobes; the lowest remaining frequency will be the upper bound on applicability of the approximate DF to an equispaced baffled volumetric array.

4. SUMMARY

Estimating the directivity of an array remains a fundamental and important aspect of array design. These estimates are used in many applications: to determine frequency regions in which an array will be ambient or self-noise limited, to determine detection ranges, and as a comparison baseline for various changes in array parameters (such as geometry, element shading coefficients, and noise distribution). It is necessary, particularly when one is trying to examine the merits of a given set of conditions over another, to have accurate estimates for directivity. The approximations presented in this report for the DFs of linear, planar, and volumetric apertures and arrays provide quick and reasonably accurate directivity estimates without having to resort to numerical integration and time-consuming computer calculations.

In figure 2, it was shown that a commonly used approximation for the directivity of a line array is valid only with omnidirectional elements and at the design frequency f_o, that is, at a *single* frequency. At other frequencies, the DF becomes a function of steering angle, and the standard approximation is inaccurate. The DF approximations derived here are more general and allow for variable steering angles and frequencies of operation.

Another useful result of this study is illustrated in figures 3 and 5, which show that highly directional array elements, such as elements having an angular response proportional to $|\cos(\Theta)|^{\nu}$, can lead to significant *decreases* in array directivity at moderate steering angles from broadside. Therefore, it may be surmised that element directivity, for most steering angles, reduces directivity, although one must bear in mind that these calculations assume a spherically isotropic noise field. Directional elements, in general, improve array gain for steering angles near broadside.

The directivity factor of a linear aperture or array depends on the first power of the effective length of the line. This results from the inability of a (vertical) line to resolve in the azimuthal direction; that is, it has a conical response region, centered on the line, within which all arrivals are treated alike. This inherent ambiguity of a line keeps the DF at moderate values. However, this lack of resolution can be partially remedied by using directional elements in the line aperture or array, leading to a modest increase in the DF.

For a planar or volumetric aperture or array, the situation is markedly improved, because simultaneous resolution in both the azimuthal and polar angles is possible. In fact, when the effective area is large compared to the squared wavelength, rather good resolution can be achieved;

this fine resolution overrides any modest directivity that individual elements may have, making the overall DF virtually independent of the individual element properties.

Baffling a planar aperture or array doubles the DF by virtue of eliminating any arrivals in the undesired hemisphere. On the other hand, a volumetric aperture or array has the inherent capability of being able to reject arrivals in an undesired hemisphere, and therefore need not employ baffling. The DF in the volumetric case is given by the same formula as for a baffled planar array, but where the effective area must be interpreted as that seen from the steering direction. In addition to steering direction, the effective area will incorporate the three-dimensional physical extent and detailed weighting of the volumetric aperture or array.

The DF approximations for linear, planar, and volumetric apertures and arrays are summarized in appendix C. Results obtained by the use of the Gaussian approximation, as well as Parseval's relation and a modification for arrays, are listed.

APPENDIX A
ALTERNATIVE INTEGRAL APPROXIMATIONS

LINEAR APERTURE

From equation (20), the amplitude response of a continuously weighted directional line aperture is given as

$$A(\theta,\phi) = \left|\sin(\theta)\sin(\phi)\right|^{v} \int_{-\infty}^{\infty} w(z)\exp\left\{ikz(\cos(\phi)-\cos(\phi_s))\right\}dz\,. \tag{A-1}$$

The value $v = 0$ corresponds to an omnidirectional element angular response. The directivity factor is again expressed as

$$DF = \frac{4\pi\left|A(\theta_s,\phi_s)\right|^2}{\int_0^{2\pi}\int_0^{\pi}\left|A(\theta,\phi)\right|^2\sin(\phi)d\phi d\theta}. \tag{A-2}$$

Then the integral which must be approximated is, as in equation (21),

$$I = \int_0^{2\pi}\left\{\sin^2(\theta)\right\}^{v}d\theta\int_0^{\pi}\left\{\sin^2(\phi)\right\}^{v}\sin(\phi)d\phi\left|\int_{-\infty}^{\infty} w(z)\exp\left\{ikz(\cos(\phi)-\cos(\phi_s))\right\}dz\right|^2. \tag{A-3}$$

Expressing the magnitude-squared as a double integral on z and ζ and letting $u = \cos(\phi)$ and $s = z - \zeta$, where ζ is a dummy variable of integration, equation (A-3) becomes

$$I = h(v)\int_{-\infty}^{\infty}\int_{-\infty}^{\infty} w(z)w(z-s)\exp\left\{-iksu_s\right\}\int_{-1}^{1}(1-u^2)^{v}\exp\left\{iksu\right\}dudzds\,, \tag{A-4}$$

where $h(v)$ is defined by equation (11). The inner integral over u in equation (A-4) may be evaluated exactly[6, p.321] yielding

$$I = h(v)\int_{-\infty}^{\infty}\int_{-\infty}^{\infty} w(z)w(z-s)\exp\left\{-iksu_s\right\}\sqrt{\pi}\,\Gamma(v+1)\left[2/ks\right]^{v+\frac{1}{2}}J_{v+1/2}(ks)dzds. \tag{A-5}$$

By using the relation $h(v) = 2\sqrt{\pi}\,\Gamma(v+1/2)/\Gamma(v+1)$ in equation (11) and the weighting autocorrelation function defined as

$$\Phi_w(s) = \int_{-\infty}^{\infty} w(z)w(z-s)dz, \tag{A-6}$$

equation (A-5) can be expressed as

$$I = 2\pi\Gamma(v+1/2)\int_{-\infty}^{\infty}\Phi_w(s)\exp\{-iks\cos(\phi_s)\}\left[2/ks\right]^{v+\frac{1}{2}}J_{v+1/2}(ks)ds. \tag{A-7}$$

However, because $\Phi_w(s)$ varies slowly with s relative to the remaining functions in equation (A-7), the following approximation obtains:

$$I \cong 2^{v+5/2}\pi\Gamma(v+1/2)\Phi_w(0)\int_0^{\infty}\frac{\cos(ks\cos(\phi_s))J_{v+1/2}(ks)}{(ks)^{v+1/2}}ds, \tag{A-8}$$

using the even character of entire function $J_\mu(z)/z^\mu$ in z. Finally, use of Erdelyi[7] yields the result

$$I \cong 4\pi^{3/2}\frac{\Gamma(v+1/2)}{k\Gamma(v+1)}\sin^{2v}(\phi_s)\,\Phi_w(0). \tag{A-9}$$

The approximate DF follows from equation (A-2) according to

$$DF \cong \frac{2L_e}{\lambda}\frac{\sqrt{\pi}\Gamma(v+1)}{\Gamma(v+1/2)}\sin^{2v}(\theta_s), \tag{A-10}$$

where L_e is the effective length of the weighting,

$$L_e = \frac{\left[\int_{-\infty}^{\infty} w(z)dz\right]^2}{\int_{-\infty}^{\infty} w^2(z)dz}. \tag{A-11}$$

In the special case of a nondirectional aperture, $\nu = 0$, equation (A-10) simplifies to the standard result

$$DF \cong \frac{2L_e}{\lambda}, \tag{A-12}$$

which is independent of the steering direction.

More generally, for arbitrary element directional response $g(\theta, \phi)$ in equation (A-1) instead of $|\sin(\theta)\sin(\phi)|^{\nu}$, the approximate DF in equation (A-10) is replaced by

$$DF \cong \frac{2L_e}{\lambda} \frac{2\pi g^2(\theta_s, \phi_s)}{\int_0^{2\pi} g^2(\theta, \phi_s) d\theta}. \tag{A-13}$$

A more direct derivation of the result in equation (A-9) may be obtained by use of Parseval's relation: from equations (22) and (23), the integral on u is, for $|u_s| = |\cos(\phi_s)| < 1$,

$$\int_{-1}^{1} \left| W\left(k(u-u_s)\right) \right|^2 du \cong \int_{-\infty}^{\infty} \left| W\left(k(u-u_s)\right) \right|^2 du = \lambda \int_{-\infty}^{\infty} w^2(z) dz = \lambda\, \Phi_w(0). \tag{A-14}$$

Then, equation (22) yields

$$I \cong h(\nu) \sin^{2\nu}(\phi_s)\, \lambda\, \Phi_w(0), \tag{A-15}$$

which is identical to equation (A-9). The same approximation for the DF, as given by equations (A-10) and (A-11), results.

PLANAR APERTURE

An alternative to expression (38) for the DF of an unbaffled planar aperture is possible through the use of Parseval's relation in two dimensions. Namely, from equations (32) and (35), there follows immediately

$$I \cong 2\left(\cos(\phi_s)\right)^{2\nu-1} \lambda^2 \iint_{-\infty}^{\infty} w^2(x,y)dxdy \tag{A-16}$$

for the denominator of equation (7). The approximate DF then readily follows as

$$DF \cong 2\pi \frac{A_e}{\lambda^2} \cos(\phi_s), \tag{A-17}$$

where the effective area of weighting $w(x,y)$ is defined as

$$A_e = \frac{\left[\iint_{-\infty}^{\infty} w(x,y)dxdy\right]^2}{\iint_{-\infty}^{\infty} w^2(x,y)dxdy}. \tag{A-18}$$

(For uniform weighting over physical lengths L_x and L_y, this definition reduces to $A_e = L_x L_y$, as noted under equation (39)).

APPENDIX B
ALTERNATIVE APPROXIMATE DIRECTIVITY FACTOR FOR EQUISPACED ARRAYS

In the main text, an approximate DF was derived for linear and planar apertures by matching the mainlobe region of the beam pattern power response with a Gaussian function. This approximate result was then extended to discrete linear and planar arrays by replacing the continuous weighting functions by sets of weighted impulses. The end results employed RMS measures of the extent of the aperture or array.

The major limitation of the Gaussian approximation is that it takes no account of the actual *sidelobe* levels of the beam pattern; that is, the Gaussian approximation matches only the three lowest-order derivatives of the response in the mainlobe region. This procedure could be extended to higher derivatives by using a more general fit, such as $\exp(-\alpha x^2)(A + Bx^4)$; however, this modification would still not take account of the distant sidelobes.

This appendix presents an alternative approximation for the DF of equispaced linear and planar arrays that does account for the sidelobes. (It does not, however, account for the grating lobes.) Then, the result is extended to equispaced volumetric arrays by means of a conjectured form. This new procedure can be thought of as an extension of Parseval's relation (which is applicable to apertures with continuous weighting) to discrete arrays with impulsive weighting. The end results will employ effective measures of the array extent.

EQUIPSACED LINEAR ARRAY

In equation (22), the double integral over angles ϕ,θ ,for the noise output power of a linear aperture, was simplified to

$$V = 2\pi \int_{-1}^{1} \left| W\left(ku - ku_s\right) \right|^2 du \,, \qquad W(v) = \int w(z) \exp(ivz) dz \,, \tag{B-1}$$

for continuous weighting $w(z)$ and $v = 0$, where steering parameter $u_s = \cos\phi_s$. For an equispaced weighted line array on the z-axis, the weighting takes the special form

$$w(z) = \sum_n w_n \, \delta(z - nd) \,, \tag{B-2}$$

leading to window function

$$W(v) = \sum_n w_n \exp(indv) \tag{B-3}$$

for all v, which has period $2\pi/d$ in v.

The integral in equation (B-1) now takes the form

$$V = 2\pi \int_{-1}^{1} \left| \sum_n w_n \exp\left(in \frac{2\pi d}{\lambda}(u - u_s) \right) \right|^2 du \,. \tag{B-4}$$

The integrand has a desired peak at $u = u_s$, along with undesired periodic grating lobes separated from u_s by multiples of λ/d. If element spacing d is less than a half-wavelength, then the period $P = \lambda/d > 2$, and all the grating lobes of $\left|W(ku - ku_s)\right|^2$ lie outside of the (-1,1) interval in u. Therefore, if the array length is much greater than a wavelength, and if the sidelobes are low level, the integration interval in equation (B-4) can be modified, leading to approximation

$$V \cong 2\pi \int_{-P/2}^{P/2} \left| \sum_n w_n \exp\left(in \frac{2\pi d}{\lambda} u \right) \right|^2 du = 2\pi \frac{\lambda}{d} \sum_n w_n^2 \,. \tag{B-5}$$

(This last quantity is the discrete analogue to Parseval's relation for apertures, which yields the integral of the squared weighting.) Use of relations (B-3) and (B-5) now yields the DF approximation for a linear equispaced array in the form

$$DF = \frac{4\pi W^2(0)}{V} \cong \frac{2d}{\lambda} N_z \,, \qquad N_z \equiv \frac{\left(\sum_n w_n \right)^2}{\sum_n w_n^2} \,. \tag{B-6}$$

The quantity N_z is the effective number of weights in real set $\{w_n\}$. (For flat weights, N_z is simply the number of elements.) If quantity dN_z is interpreted as the effective length L_e of the discrete array, relation (B-6) for the approximate DF takes the same form as for a linear aperture, namely, $2\,L_e/\lambda$.

For elements with amplitude directionality $|\sin\theta \sin\phi|$, relation (B-6) is somewhat modified, to the extent that the factor of 2 in the DF is replaced by 4 $\sin^2 \theta_s$. The factor N_z is unchanged.

Although the derivation above presumed $d/\lambda < 1/2$, result (B-6) is actually valid for the broader region $d/\lambda < 1/(1+|u_s|)$. This is due to the fact that the nearest grating lobe does not yet affect the noise integral for this region of values of d/λ.

EQUISPACED PLANAR ARRAY

In equation (34), the double integral over angles ϕ,θ, for the noise output power of a baffled planar aperture in the *xy*-plane, was simplified (for $v = 0$) to

$$V \cong \frac{1}{w_s} \iint_{C_1} \left| W\left(ku - ku_s\,,\, kv - kv_s\right) \right|^2 du dv\,, \tag{B-7}$$

where C_1 is a unit circle centered at the origin, steering parameter $w_s = \cos\phi_s > 0$, and window

$$W(u,v) = \iint w(x,y)\exp(iux + ivy)dxdy \tag{B-8}$$

for all u,v, which depends on continuous two-dimensional weighting $w(x, y)$. For an equispaced weighted planar array, the weighting takes the special form

$$w(x,y) = \sum_{nm} w_{nm}\, \delta\left(x - nd_x\right) \delta\left(y - md_y\right), \tag{B-9}$$

leading to window function

$$W(u,v) = \sum_{nm} w_{nm} \exp\left(ind_x u + imd_y v\right) \tag{B-10}$$

for all u,v, which has period $2\pi/d_x$ in u and period $2\pi/d_y$ in v.

Substitution of equation (B-10) in equation (B-7) yields

$$V = \frac{1}{w_s} \iint_{C_1} \left| \sum_{nm} w_{nm} \exp\left(in \frac{2\pi d_x}{\lambda}(u - u_s) + im \frac{2\pi d_y}{\lambda}(v - v_s) \right) \right|^2 du dv . \qquad \text{(B-11)}$$

The integrand has a desired peak at $u = u_s, v = v_s$, along with undesired periodic grating lobes separated from u_s, v_s by multiples of $\lambda/d_x, \lambda/d_y$ in u,v, respectively. If element spacings d_x and d_y are both less than a half-wavelength, then the periods λ/d_x and λ/d_y are both greater than 2, and all the grating lobes of $\left| W(ku - ku_s, kv - kv_s) \right|^2$ lie outside of the unit circle C_1 in the uv-plane. Therefore, if the array lengths in the x- and y-directions are both much greater than a wavelength, and if the sidelobes are low level, the integration region in equation (B-11) can be modified, leading to approximation

$$V \cong \frac{1}{w_s} \iint_{R} \left| \sum_{nm} w_{nm} \exp\left(in \frac{2\pi d_x}{\lambda} u + im \frac{2\pi d_y}{\lambda} v \right) \right|^2 du dv$$

$$= \frac{1}{w_S} \iint_{R} \sum_{nm} \sum_{kj} w_{nm} w_{kj} \exp\left(i(n-k) \frac{2\pi d_x}{\lambda} u + i(m-j) \frac{2\pi d_y}{\lambda} v \right) du dv \qquad \text{(B-12)}$$

$$= \frac{\lambda^2}{w_s d_x d_y} \sum_{nm} w_{nm}^2 ,$$

where R is a rectangle of size $\pm\lambda/(2d_x)$ by $\pm\lambda/(2d_y)$, centered at the origin of the uv-plane. (The last quantity in equation (B-12) is the discrete analogue to Parseval's two-dimensional relation for apertures, which yields the integral of the squared weighting $w(x, y)$.) Use of relations (B-8) and (B-12) now yields the DF approximation for an equispaced baffled planar array as

$$DF = \frac{4\pi W^2(0,0)}{V} \cong \left| \cos\phi_s \right| \frac{4\pi d_x d_y}{\lambda^2} N_{xy} , \qquad N_{xy} \equiv \frac{\left(\sum_{nm} w_{nm} \right)^2}{\sum_{nm} w_{nm}^2} . \qquad \text{(B-13)}$$

The quantity N_{xy} is the effective number of weights in two-dimensional real set $\{w_{nm}\}$. (For flat weights, N_{xy} is simply the total number of elements employed in the xy-plane.) If the quantity $d_x d_y N_{xy}$ is interpreted as the effective area A_{xy} of the discrete planar array, relation (B-13) for the

approximate DF of a baffled planar array takes the same form as for a baffled planar aperture, namely $|\cos\phi_s| 4\pi A_{xy}/\lambda^2$. An alternative expression for the DF of a baffled planar aperture is

$$DF \cong 4\pi \frac{A_e}{\lambda^2}, \tag{B-14}$$

where $A_e = |\cos\phi_s| A_{xy}$ is the effective area of the planar aperture, *as seen from the steering direction* θ_s, ϕ_s.

For elements with moderate amplitude directionality, relation (B-13) for the approximate DF is unchanged because a two-dimensional array can have simultaneous fine resolution ability in both the azimuthal and polar angles. This fine resolution dominates the relative slowly varying selectivity of the individual element directionality, effectively factoring it out of the double integral on θ,ϕ, with the element directionality value taken at the steering angle θ_s, ϕ_s.

Although the derivation above presumed $d_x < \lambda/2$ and $d_y < \lambda/2$, result (B-13) is actually valid for the broader region where

$$\left(u_s + I\frac{\lambda}{d_x}\right)^2 + \left(v_s + J\frac{\lambda}{d_y}\right)^2 > 1 \tag{B-15}$$

for *all* integers I and J equal to -1, 0, +1, except that $I, J = 0, 0$ is disallowed. Restriction (B-15) guarantees that none of the grating lobes in equation (B-11) lie inside the unit circle C_1; this is consistent with the rectangular replacement used in approximation (B-12), which guaranteed the exclusion of all grating lobes from the rectangular integration region.

EQUISPACED VOLUMETRIC ARRAY

The authors have been unable to discover how to extend the arguments above to a volumetric aperture or equispaced array; accordingly, conjectured forms for the DF of volumetric apertures and arrays are constructed based on the earlier forms in this appendix for the approximate DFs in the planar case.

Whereas a planar aperture or array occupies only the *xy*-plane, a volumetric aperture or array occupies the third dimension, namely *z*. This gives the steered volumetric amplitude response the capability to reject responses in an undesired hemisphere, whether it is baffled or not. Therefore, the *baffled* planar DF result in equation (B-14) should furnish the model form for the three-dimensional cases (whether baffled or not), namely

$$DF \cong 4\pi \frac{A_e}{\lambda^2}, \tag{B-16}$$

where A_e is now the effective area of the volumetric aperture or array, *as seen from the steering direction* $\theta_s \phi_s$.

In particular, guided by the Gaussian form in equations (59) through (62), there follows, for a volumetric aperture,

$$A_e = \left(w_s^2 A_{xy}^2 + v_s^2 A_{xz}^2 + u_s^2 A_{yz}^2 \right)^{1/2}, \tag{B-17}$$

where the *projected* effective areas are defined in terms of the three-dimensional aperture weighting w(x, y, z) according to

$$A_{xy} = \frac{\left(\iint w_{xy}(x,y)dxdy \right)^2}{\iint w_{xy}^2(x,y)dxdy}, \qquad w_{xy}(x,y) = \int w(x,y,z)dz, \quad \text{etc.} \tag{B-18}$$

For an equispaced volumetric *array* with discrete three-dimensional weighting $w(n,m,k)$ and spacings d_x, d_y, d_z, aproximate DF (B-16) is still appropriate, but where the effective area is now represented as

$$A_e = \left(w_s^2 N_{xy}^2 d_x^2 d_y^2 + v_s^2 N_{xz}^2 d_x^2 d_z^2 + u_s^2 N_{yz}^2 d_y^2 d_z^2 \right)^{1/2}. \qquad \text{(B-19)}$$

The *projected* effective numbers of elements here are given in terms of the three-dimensional weighting $\{w(n,m,k)\}$ as

$$N_{xy} = \frac{\left(\sum_{nm} w_{xy}(n,m) \right)^2}{\sum_{nm} w_{xy}^2(n,m)}, \qquad w_{xy}(n,m) = \sum_k w(n,m,k), \qquad \text{etc.} \qquad \text{(B-20)}$$

Although there is only one form, namely equation (B-16) with definitions (B-19) and (B-20), for the approximate DF of an equispaced volumetric array, this form has different ranges of applicability, depending on whether baffling is used. The approximate DF takes no account of grating lobes, whereas actual arrays are always subject to the effects of grating lobes. This is evident in figure 14 where the agreement of the approximate DF with the exact baffled DF is excellent up to $f/f_o = 1.8$, whereas the agreement with the exact unbaffled DF holds only up to $f/f_o = 0.9$. This is due to the fact that baffling suppresses all the lower-hemisphere grating lobes; the dip in the unbaffled DF near $f/f_o = 1$ is due to a lower-hemisphere grating lobe that is responding to undesired noise arrivals. However, it should be noted that for frequencies $1.1 < f/f_o < 1.7$, the approximate DF again agrees with the exact unbaffled DF; this occurs because this particular grating lobe in figure 14 only contributes in the neighborhood of $f/f_o = 1$.

The general frequencies at which an equispaced unbaffled volumetric array is subject to a grating lobe are

$$\frac{f}{f_o} = \frac{I^2 + J^2 + K^2}{\left| u_s I + v_s J + w_s K \right|}, \qquad \text{(B-21)}$$

where I, J, K are positive and negative integers, not all equal to zero. The lowest problematical frequency was given earlier in equation (75).

For an equispaced *baffled* volumetric array, not all the frequencies in equation (B-21) lead to grating lobes. To determine which frequencies are relevant, a search over all the small integer

values for I, J, K, such as 0, ±1, ±2, must first be conducted. Then, those cases corresponding to negative values of $w_s + K\ 2f_o/f$ must be discarded, because they correspond to lower-hemisphere grating lobes, which will not be active in a baffled application. The remaining cases constitute valid grating lobes; the lowest remaining frequency furnishes the upper bound on applicability of the approximate DF to an equispaced baffled volumetric array.

APPENDIX C
SUMMARY OF FORMULAS FOR APPROXIMATE DIRECTIVITY FACTOR

The approximate relations for the DF are listed below. In each case, the Gaussian results are presented first; then, the results of the alternative method employing Parseval's relation, or a modification for equispaced arrays, are summarized.

LINEAR APERTURE

$$DF = 4\sqrt{\pi}\,\frac{m}{\lambda}\,\frac{2\pi g^2(\theta_s,\phi_s)}{\int_0^{2\pi} g^2(\theta,\phi_s)\,d\theta}. \tag{C-1}$$

$$m = \left(\frac{\int_{-\infty}^{\infty} z^2 w(z)\,dz}{\int_{-\infty}^{\infty} w(z)\,dz}\right)^{1/2}. \tag{C-2}$$

$$DF = \frac{2L_e}{\lambda}\,\frac{2\pi g^2(\theta_s,\phi_s)}{\int_0^{2\pi} g^2(\theta,\phi_s)\,d\theta}. \tag{C-3}$$

$$L_e = \frac{\left[\int_{-\infty}^{\infty} w(z)\,dz\right]^2}{\int_{-\infty}^{\infty} w^2(z)\,dz}. \tag{C-4}$$

LINEAR ARRAY

$$DF = \frac{4\sqrt{\pi}}{\lambda}\,\frac{\left\{\sum_{n=1}^{N} w_n z_n^2\right\}^{1/2}}{\left\{\sum_{n=1}^{N} w_n\right\}^{1/2}}. \tag{C-5}$$

$$DF = \frac{2d}{\lambda} N_z. \tag{C-6}$$

$$N_z = \frac{\left(\sum_n w_n\right)^2}{\sum_n w_n^2}. \tag{C-7}$$

PLANAR APERTURE (UNBAFFLED)

$$DF = 8\pi^2 \cos(\phi_s)\frac{m_x m_y}{\lambda^2}. \tag{C-8}$$

$$m_x = \left(\frac{\int_{-\infty}^{\infty}\int_{-\infty}^{\infty} x^2 w(x,y)dxdy}{\int_{-\infty}^{\infty}\int_{-\infty}^{\infty} w(x,y)dxdy}\right)^{1/2}. \tag{C-9}$$

$$DF = 2\pi\frac{A_e}{\lambda^2}\cos(\phi_s). \tag{C-10}$$

$$A_e = \frac{\left[\iint_{-\infty}^{\infty} w(x,y)dxdy\right]^2}{\iint_{-\infty}^{\infty} w^2(x,y)dxdy}. \tag{C-11}$$

PLANAR ARRAY (UNBAFFLED)

$$DF = \frac{8\pi^2 d_x d_y \cos(\phi_s)}{\lambda^2}\frac{\left\{\sum_{n=1}^{N}\sum_{m=1}^{M} w_{nm}\left[n-\frac{N+1}{2}\right]^2\right\}^{1/2}\left\{\sum_{n=1}^{N}\sum_{m=1}^{M} w_{nm}\left[m-\frac{M+1}{2}\right]^2\right\}^{1/2}}{\sum_{n=1}^{N}\sum_{m=1}^{M} w_{nm}}. \tag{C-12}$$

$$DF = \left|\cos\phi_s\right|\frac{2\pi d_x d_y}{\lambda^2}N_{xy}. \tag{C-13}$$

$$N_{xy} \equiv \frac{\left(\sum_{nm} w_{nm}\right)^2}{\sum_{nm} w_{nm}^2}. \tag{C-14}$$

VOLUMETRIC APERTURE

$$DF = \frac{16\pi^2}{\lambda^2}\sqrt{m_x^2 m_y^2 \cos^2(\phi_s) + m_x^2 m_z^2 \sin^2(\phi_s)\sin^2(\theta_s) + m_y^2 m_z^2 \sin^2(\phi_s)\cos^2(\theta_s)}\,. \tag{C-15}$$

$$m_x = \left(\frac{\int_{-\infty}^{\infty}\int_{-\infty}^{\infty}\int_{-\infty}^{\infty} x^2 \overline{w}(x,y,z)\,dxdydz}{\int_{-\infty}^{\infty}\int_{-\infty}^{\infty}\int_{-\infty}^{\infty} \overline{w}(x,y,z)\,dxdydz} \right)^{1/2}. \tag{C-16}$$

$$DF = 4\pi \frac{A_e}{\lambda^2}. \tag{C-17}$$

$$A_e = \left(w_s^2 A_{xy}^2 + v_s^2 A_{xz}^2 + u_s^2 A_{yz}^2 \right)^{1/2}. \tag{C-18}$$

$$A_{xy} = \frac{\left(\iint w_{xy}(x,y)\,dxdy \right)^2}{\iint w_{xy}^2(x,y)\,dxdy}, \qquad w_{xy}(x,y) = \int w(x,y,z)\,dz, \quad \text{etc.} \tag{C-19}$$

VOLUMETRIC ARRAY

$$DF = \frac{16\pi^2}{\lambda^2}\sqrt{m_x^2 m_y^2 \cos^2(\phi_s) + m_x^2 m_z^2 \sin^2(\phi_s)\sin^2(\theta_s) + m_y^2 m_z^2 \sin^2(\phi_s)\cos^2(\theta_s)}\,. \tag{C-20}$$

$$m_x = \left(\frac{\sum_t \overline{w}_t x_t^2}{\sum_t \overline{w}_t} \right)^{1/2} \text{; see equation (66).} \tag{C-21}$$

$$DF = 4\pi \frac{A_e}{\lambda^2}. \tag{C-22}$$

$$A_e = \left(w_s^2 N_{xy}^2 d_x^2 d_y^2 + v_s^2 N_{xz}^2 d_x^2 d_z^2 + u_s^2 N_{yz}^2 d_y^2 d_z^2 \right)^{1/2}. \tag{C-23}$$

$$N_{xy} = \frac{\left(\sum_{nm} w_{xy}(n,m) \right)^2}{\sum_{nm} w_{xy}^2(n,m)}, \qquad w_{xy}(n,m) = \sum_k w(n,m,k), \qquad \text{etc.} \tag{C-24}$$

OTHER ARRAY GEOMETRIES

Directivity approximations for many additional array geometries have been derived in the past.[8] DFs for some other common types are

$$DF_{ring\ array} \cong \frac{2\pi d/\lambda}{1+\sqrt{\frac{\lambda}{\pi^2 d}}\sin\left(\frac{2\pi d}{\lambda}-\frac{\pi}{4}\right)}, \tag{C-25}$$

where d is the diameter of the continuous ring aperture. For $d/\lambda >> 1$, the directivity factor approaches $DF_{ring\ array} \to 2\pi d/\lambda$, which increases linearly with d. Compare this behavior with figures 10 and 11 for a semicircular array.

For a flat circular plate of diameter d,

$$DF_{circular\ plate} \cong \frac{(\pi d/\lambda)^2}{1-\frac{\lambda}{\pi d}\sqrt{\frac{\lambda}{\pi^2 d}}\sin\left(\frac{2\pi d}{\lambda}-\frac{\pi}{4}\right)}. \tag{C-26}$$

When $d/\lambda >> 1$, this equation leads to the well-known approximation for a piston in a rigid baffle, namely, $DF_{piston} \cong \left(\pi d/\lambda\right)^2 = 4\pi\, A_e/\lambda^2$.

REFERENCES

1. R.J. Bobber, "Approximations to the Directivity Index," NRL Report 7750, Naval Research Laboratory, Washington, D.C., May 1974.

2. C.T. Molloy, "Calculation of the Directivity Index for Various Types of Radiators," *Journal of the Acoustical Society of America*, vol. 20, 1948, pp. 387-405.

3. A.H. Nuttall and B.A. Cray, "Efficient Calculation of Directivity Indices for Certain Three-Dimensional Arrays," NUWC-NPT Technical Report 11,129, Naval Undersea Warfare Center Division, Newport, RI, 26 July 1996.\

4. I.S. Gradshetyn and I.M. Ryzhik, *Tables of Integrals, Series, and Products*, Academic Press, New York, 1980.

5. M. Abramowitz and I.A. Stegun, *Handbook of Mathematical Functions*, U.S. Department of Commerce, National Bureau of Standards, Washington, D.C., 1972, p. 256, equation (6.1.18).

6. V.C. Anderson and J.C. Munson, "Directivity of Spherical Receiving Arrays," *Journal of the Acoustical Society of America*, vol. 35, no. 8, 1963, pp. 1162-1168.

7. A. Erdelyi, *Tables of Integral Transforms*, Volume 1, McGraw-Hill, New York, 1954, p. 44, equation (9).

8. J.W. Horton, *Fundamentals of Sonar*, United States Naval Institute, Library of Congress Catalog Card No. 56-10026, 1960.

INITIAL DISTRIBUTION LIST

Addressee	No. of Copies
Center for Naval Analyses	1
Defense Technical Information Center	12
Office of the Chief of Naval Operations (N871—J.Schuster)	1
Office of Naval Research (ONR-321SS—K. Dial, S. Littlefield; ONR-321US—J. Tague)	3
Program Executive Officer for Undersea Warfare (ASTO—J. Thomson, M. Traweek)	2
Bolt, Beranek and Newman (N. Martin, R. Brown) Contract No. N66604-95-D-0221	2
Litton Guidance and Control Systems (S. Martin) Contract No. N66604-91-C-2841	1